発表者氏名	論文タイトル名	発表誌名	巻・頁・出版名
Zhang, X., Koldzix, D.J., Izikson, L., Reddy, J., Nazareno, R. F., Sakaguchi, S., Kuchroo, V. K., and Weiner, H. L.	IL-10 is involved in the suppression of experimental autoimmune encephalomyelitis by $CD25^+CD4^+$ regulatory T cells.	Int. Immunology.	16: 1-8, 2004.
Fehervari, Z., and Sakaguchi, S.	Development and function of $CD25^+CD4^+$ regulatory T cells.	Curr. Opinion in Immunol.	16:203-208, 2004.
Fehervari, Z. and Sakaguchi, S.	A paragon of self-tolerance:Regulatory T cells and the control of immune responses.	Arthritis Res. Ther.	6: 19-25, 2004.
Sakaguchi, S.	Naturally arising *Foxp3*-expressing $CD25^+CD4^+$ regulatory T cells in immunologic tolerance to self and non-self.	Nature Immunol.	In press.
Chai, J-G., Xue, S., Coe, D., Addey, C., Bartok, I., Scott, D., Simpson, E., Stauss, H. J., Hori, S., Sakaguchi, S., and Dyson, J. P.	T regulatory cells, derived from naïve $CD4^+CD25^-$ T cells by in vitro Foxp3 gene transfer, can induce transplantation tolerance.	Transplantation.	In press.
Sakaguchi, S., and Sakaguchi, N.	History of $CD25^+CD4^+$ regulatory T cells.	Progress in Inflammation Research.	In press.
Nomura, T., and Sakaguchi, S.	Regulatory T cells in tumor immunity.	Current Topics in Microbiology and Immunology.	In press.
Sakaguchi, S.	Preface: Regulatory T cells in autoimmune diseases.	Int. Rev. Immunol.	In press.
Sakaguchi, S. and Sakaguchi, N.	Regulatory T cells in self-tolerance and autoimmune diseases.	Int. Rev. Immunol.	In press.
Fehervari, Z. and Sakaguchi, S.	A common basis of self-tolerance and transplantation tolerance: a simple way of inducing transplantation tolerance with naturally arising $CD25^+CD4^+$ regulatory T cells.	Philosophical Transactions: Biological Sciences.	In press.
Fehervari, Z. and Sakaguchi, S.	T lymphocytes: Regulatory.	Nature Encyclopedia of Life Sciences.	In press.
Matsubara, Y., Hori, T., Morita, R., Sakaguchi, S., and Uchiyama, T.	Phenotypic and functional relationship between adult T cell leukemia and regulatory T cells.	Leukemia.	In press.
Setoguchi, R., Hori, S., Takahashi, T., and Sakaguchi, S.	A crucial role of IL-2 in the homeostatic maintenance of $CD25^+CD4^+$ regulatory T cells: induction of autoimmune disease by neutralization of IL-2.	J. Exp. Med.	In press.
Yoshitomi, H., Sakaguchi, N., Brown, G., Tagami, T., Sakihama, T., Nomura, T., Akira, S., Gordon, S., Nakamura, T., and Sakaguchi, S.	Environmental stimulation of innate immunity triggers chronic arthritis in mice genetically prone to produce arthritogenic autoimmune T cells: a key role of fungal β-glucans and their receptor Dectin-1.	J. Exp. Med.	In press.
田中良哉，中山田真吾.	β_1インテグリンシグナル伝達と SLE.	炎症と免疫 (2005).	13, 87-94.
田中良哉.	ステロイドの効果と注意点.	痛みと臨床 (2005).	5, 34-41.
Okada Y, Tanaka Y.	Immune signals in the context of secondary osteoporosis.	Histol Histopathol (2004).	19, 863-866.
Nakayamada S, Okada S, Saito K, Tanaka Y.	Etidronate prevents high-dose glucocorticoid-induced bone loss in premenopausal individuals with systemic autoimmune diseases.	J Rheumatol (2004).	31, 163-166.

発表者氏名	論文タイトル名	発表誌名	巻・頁・出版名
Saito K, Nakayamada S, Nakano K, Tokunaga M, Tsujimura S, Nakatsuka K, Adachi T, Tanaka Y.	Detection of *Pneumocystis carinii* by DNA amplification in patients with connective tissue diseases: Reevaluation of clinical features of *P. carinii* pneumonia in rheumatic diseases.	Rheumatology (2004).	43, 479-485.
Okada Y, Tsukada J, Nakano K, Tonai S, Mine S, Tanaka Y.	Macrophage inflammatory protein-1αinduces hypercalcemia in adult T-cell leukemia.	J Bone Miner Res (2004).	19, 1105-1111.
Nakano K, Okada Y, Saito K, Tanaka Y.	Fibroblast growth factor-2 induces receptor activator of nuclear factor kappa B ligand expression and osteoclast maturation by binding to heparan sulfate proteoglycan on rheumatoid synovial fibroblasts.	Arthritis Rheum (2004).	50, 2450-2458.
Tsujimura S, Saito K, Nakayamada S, Nakano K, Tsukada J, Kohno K, Tanaka Y.	Transcriptional regulation of multidrug resistance-1 gene by interleukin-2 in lymphocytes.	Genes Cells (2004).	9, 1265-1273.
Kato N, Fujimoto H, Yoda A, Oishi I, Matsuura N, Kondo T, Tsukada J, Tanaka Y, Imamura M, Minami Y.	Regulation of Chk2 gene expression in lymphoid malignancies: involvement of epigenetic mechnisims in Hodgkin's lymphoma cell lines.	Cell Death Differ (2004).	11: S153-S161.
Ehara Y, Sakurai D, Tsuchiya N, Nakano K, Tanaka Y, Yamaguchi A, Tokunaga K.	Follistatin-related protein gene (FRP) is expressed in the synovial tissues of rheumatoid arthritis, but its polymorphisms are not associated with genetic susceptibility.	Clin Exp Rheuamtol (2004).	22: 707-712.
Tanikawa T, Okada Y, Azuma T, Fukushima A, Kawahara C, Tanaka Y.	Adult-onset idiopathic progressive acro-osteolysis with proximal symphalangism.	J Bone Miner Res (2004).	19, 165-167.
Kawahara C, Okada Y, Tanikawa T, Fukushima A, Misawa H, Tanaka Y.	Severe hypercalcemia and hypernatremia associated with calcipotriol for treatment of psoriasis.	J Bone Miner Metabolism (2004).	22, 159-162.
Kanda K, Okada Y, Tanikawa T, Morita E, Tsurudome Y, Konishi T, Tanaka Y.	A rare case of primary hyperparathyroidism with clear cell adenoma.	Endorine J (2004).	51, 207-212.
Higashi T, Tsukada J, Kato C, Iwashige A, Mizobe T, Machida S, Morimoto H, Ogawa R, Toda T, Tanaka Y.	Imatinib mesylate-sensitive blast crisis immediately after discontinuation of imatinib mesylate therapy in chronic myelogenous leukemia.	Am J Hematol (2004).	76: 275-278.
三澤晴雄，岡田洋右，神田加寿子，森田恵美子，田中良哉.	当科における糖尿病初期治療と血糖コントロール状況の変遷.	臨床と研究 (2004).	81, 111-114.
毛利文彦，塚田順一，森本浩章，東丈　裕，溝部貴光，太田貴徳，窪田　歩，戸田陽子，小川亮介，田中良哉.	成人T細胞白血病における高カルシウム血症に対するビスホスフォネートの有効性.	癌の臨床 (2004).	50, 731-736.
三澤晴雄，岡田洋右，神田加壽子，森田恵美子，田中良哉.	軽症2型糖尿病に対するナテグリニドまたはボグリボースの使用に関する臨床的相違.	Diabetes Frontier (2004).	15, 717-720.
田中良哉.	抗CD20抗体.	Current Therapy (2004).	22, 53-58.
名和田雅夫，齋藤和義，藤井幸一，徳永美貴子，塚田順一，田中良哉.	抗CD20抗体療法.	内科 (2004).	93, 319-325.
田中良哉.	免疫学的生物製剤をいかに膠原病に適応するか.	Molecular Medicine (2004).	41, 204-209.
田中良哉.	CD20を標的としたSLE等の自己免疫疾患の分子治療.	医学のあゆみ (2004).	208, 349-354.
田中良哉.	炎症細胞の遊走のメカニズム.	アレルギーの臨床 (2004).	24, 239-243.
田中良哉.	混合性結合組織病.	臨床と研究 (2004).	81, 63-66.

発表者氏名	論文タイトル名	発表誌名	巻・頁・出版名
田中良哉.	抗 CD20 抗体による自己免疫疾患の治療.	日本臨床免疫学会雑誌 (2004).	27, 28-33.
田中良哉.	抗 CD20 抗体.	分子リウマチ (2004).	1, 32-38.
齋藤和義，田中良哉.	膠原病疾患に併発するカリニ肺炎の早期診断と 1 次予防.	九州リウマチ (2004).	23, 134-138.
岡田洋右，田中良哉.	産業医から見た糖尿病治療の留意点：早期発見と早期治療.	新薬と治療 (2004).	54, 15-17.
田中良哉.	関節リウマチと全身性エリテマトーデスの治療への抗体医薬の導入.	血液・腫瘍科 (2004).	48, 523-531.
田中良哉.	骨芽細胞上の接着分子発現と活性の制御.	臨床免疫 (2004).	41, 538-544.
岡田洋右，田中良哉.	膠原病患者に於けるステロイド性骨粗鬆症発症の一次予防の検討.	Osteoporosis Japan (2004).	12, 321-322.
田中良哉.	抗リウマチ薬 ― 最近の動向.	医学のあゆみ (2004).	209, 821-826.
田中良哉，塚田順一.	CD20 を標的とした悪性リンパ腫, SLE, 関節リウマチの治療.	現代医療 (2004).	36, 1561-1567.
田中良哉，辻村静代.	P-糖蛋白質に対するシクロスポリンの作用：薬剤抵抗性の克服.	医薬ジャーナル (2004).	40, 178-182.
田中良哉.	MMP（マトリックスメタロプロテアーゼ）に対するシクロスポリンの作用.	医薬ジャーナル (2004).	40, 188-193.
田中良哉.	自己免疫疾患とケモカイン.	臨床化学 (2004).	33, 73-78.
田中良哉.	抗 CD20 抗体による SLE の治療.	リウマチ科 (2004).	31, 559-565.
田中良哉，中山田真吾，岡田洋右.	ビスホスフォネート製剤によるステロイド性骨粗鬆症の一次予防.	DENTAL DIAMOND (2004).	29, 68-69.
田中良哉.	免疫シグナルと続発性骨粗鬆症の病態機構.	日本整形外科学会雑誌 (2004).	78, 411-416.
田中良哉，齋藤和義.	膠原病に於ける日和見感染症とその対策.	日本内科学会雑誌 (2004).	93, 1654-1659.
中山田真吾，田中良哉.	SLE 患者 T 細胞活性化における CD29（β1 インテグリン）-FAK シグナル伝達系の役割.	分子リウマチ (2004).	1, 192-198.
田中良哉.	ステロイド療法とその副作用対策.	日本臨床 (2004).	62, 1867-1872.
田中良哉.	生物学的製剤(リツキシマブを中心に).	医学のあゆみ (2004).	210, 1034-1039.
田中良哉.	抗リウマチ薬.	予防医学 (2004).	34, 99-105.
田中良哉.	膠原病・リウマチの治療：薬が効かなくなったとき.	Medical Practice (2004).	21, 1753.
田中良哉，塚田順一.	接着分子と転移.	血液・腫瘍科 (2004).	49, S241-S247.
田中良哉，岡田洋右.	ランゲルハンス細胞組織球症.	Molecular medicine (2004).	41, 1382-1386.
辻村静代，齋藤和義，河野公俊，田中良哉.	SLE における多剤抵抗性遺伝子発現とその制御.	臨床免疫 (2004).	42, 442-447.
中山田真吾，田中良哉.	滑膜増殖における Rho シグナルの関与とその人為的制御.	臨床免疫 (2004).	42, 547-552.
岡崎 亮，田中良哉，田中郁子，竹内靖博.	ステロイド骨粗鬆症の現状と対策.	medicina (2004).	41, 2081-2093.
福島あゆみ，岡田洋右，谷川隆久，森田恵美子，田中良哉.	Propylthiouracil による薬剤性血小板減少と特発性血小板減少性紫斑病が合併したバセドウ病の 1 例.	内科 (2004).	93: 189-192.
辻村静代，斎藤和義，徳永美貴子，中塚敬輔，中山田真吾，中野和久，澤向範文，名和田雅夫，田中良哉.	慢性 C 型肝炎に伴うクリオグロブリン血症にて増悪した関節症状に IFN-α 療法が奏効した RA の一例.	日本臨床免疫学会雑誌 (2004).	27, 48-53.

発表者氏名	論文タイトル名	発表誌名	巻・頁・出版名
三澤晴雄，岡田洋右，谷川隆久，福島あゆみ，廣瀬暁子，河原智恵，神田加壽子，森田恵美子，田中良哉.	甲状腺機能正常化後も高インスリン血症の関与が疑われる周期性四肢麻痺を繰り返したバセドウ病の1例.	糖尿病 (2004).	47, 133-136.
福島あゆみ，岡田洋右，廣瀬暁子，河原智恵，三澤晴雄，中井美穂，谷川隆久，森田恵美子，神田加壽子，田中良哉.	ガチフロキサシンにより血糖コントロールが増悪した2型糖尿病の1例.	プラクティス (2004).	21, 201-206.
河野一郎，塚田順一，戸田陽子，小川亮介，東丈　裕，岩重淳司，太田貴徳，窪田　歩，溝部貴光，森本浩章，町田真一郎，田中良哉.	同種末梢血肝細胞移植後，インターフェロンα併用ドナーリンパ球輸注にて寛解となった治療抵抗性び慢性大細胞型B細胞リンパ腫.	臨床血液 (2004).	45, 155-160.
峯信一郎，田中良哉.	発症から自然軽快までの経過が追えたCronkhite-Canada症候群の1例.	産業医科大学雑誌 (2004).	26, 245-251.
栗田智子，松浦祐介，田中真由美，倉橋敦也，柏村正道，中野和久，田中良哉.	多発性血栓塞栓症から卵巣明細胞腺癌が発見された1症例.	産科と婦人科 (2004).	71, 677-681.
藤本良士，岡田洋右，岸川博史，神田加壽子，森田恵美子，田中良哉.	膵体尾部切除後にに発症したインスリン抵抗性を主因とした糖尿病の一例.	臨床と研究 (2004).	81: 1331-1333.
澤向範文，斎藤和義，中塚敬輔，藤井幸一，中山田真吾，藤井裕子，中野和久，徳永美貴子，辻村静代，名和田雅夫，吾妻妙子，田中良哉.	著明な大動脈弁・僧帽弁破壊により急性心不全を呈した顕微鏡的多発血管炎の一症例.	九州リウマチ (2004).	24, 93-98.
神田加壽子，岡田洋右，中井美穂，森田恵美子，田中良哉.	Crohn病再燃時に発症したバセドウ病の一例.	内科 (2004).	94, 397-399.
徳永美貴子，斎藤和義，中塚敬輔，中山田真吾，中野和久，辻村静代，大田俊行，田中良哉.	ループス脊髄炎による排尿障害並びにループス精神病にIV-CYが有効であった一症例.	日本臨床免疫学会雑誌 (2004).	27, 338-344.
河原哲也，岡田洋右，広瀬暁子，谷川隆久，神田加壽子，田中良哉.	グリチルリチンによる偽性アルドステロン症にて心停止を来たした一症例.	臨床と研究 (2004).	81, 1825-1828.
岸川博文，岡田洋右，広瀬暁子，河原哲也，三澤晴雄，谷川隆久，神田加壽子，森田恵美子，田中良哉.	Loxoprofen sodiumが誘引と思われるインスリン自己免疫症候群の1例.	糖尿病 (2004).	47, 851-854.
Tokunaga M, Fujii K, Saito K, Nakayamada S, Tsujimura S, Nawata M, Tanaka Y.	Down-regulation of CD40 and CD80 on B cells in patients with life-threatening systemic lupus erythematosus after successful treatment with rituximab.	Rheumatology.	in press.
Tsujimura S, Saito K, Tokunaga M, Nakatsuka K, Nakayamada S, Nakano K, Tanaka Y.	Overcoming treatment unresponsiveness mediated by P-glycoprotein overexpression on lymphocytes in refractory active systemic lupus erythematosus.	Mod Rheumatol.	in press.
Sakuma-Zenke M, Sakai A, Nakayamada S, Kunugita N, Uchida S, Tanaka S, Mori T, Tanaka Y, T Nakamura.	Reduced expression of platelet endothelial cell adhesion molecule-1 in bone marrow cells in mice after unloading.	J Bone Miner Res.	in press.
Nakayamada S, Kurose K, Saito K, Mogami A, Tanaka Y.	Small GTP-binding protein rho-mediated signaling promotes proliferation of rheumatoid synovial fibroblasts.	Arthritis Res Ther.	in press.
Tanaka Y, Nakayamada S, Okada Y.	Osteoblasts and osteoclasts in bone remodeling and inflammation.	Current Drug targets-inflammation and allergy.	in press.
Tsujimura S, Saito K, Nakayamada S, Nakano K, Tanaka Y.	Clinical relevance of expression of P-glycoprotein on peripheral lymphocytes to steroid resistance in systemic lupus erythematosus.	Arthritis Rheum.	in press.

書籍

著者氏名	論文タイトル名	書籍全体の編集者名	書籍名	出版社名・出版地	出版年・ページ
Atsumi,T.,Matsuura, E.,Koike, T.	Immunology of anti-phospholipid antibodies and cofactors.	Lahita RG ed.	Systemic Lupus Erythematosus 4rd edition.	Harcourt Brace & Campany.	1081-1105.2004.
佐藤準一, 山村　隆.	サイトカインの生理活性-神経系. Overview.	宮坂　信之, 宮島篤	別冊・医学のあゆみ. サイトカイン –state of arts.	医歯薬出版（東京）	pp 119-122, 2004.
宮本勝一, 山村　隆.	サイトカインの病態への関与. 多発性硬化症.	宮坂　信之, 宮島篤	別冊・医学のあゆみ. サイトカイン –state of arts.	医歯薬出版（東京）	pp 245-247, 2004.
田中良哉.	成人発症スチル病.	山口徹, 北原光夫編	今日の治療指針 2005 年版.	医学書院	586-587 頁 (2005).
田中良哉.	抗 CD20 抗体.	宮坂信之編	関節リウマチ：成因研究から治療の新時代へ.	日本臨床社	544-548 頁 (2005).
田中良哉.	ステロイド薬.	宮坂信之編	関節リウマチ：成因研究から治療の新時代へ.	日本臨床社	468-472 頁 (2005).
田中良哉.	炎症細胞遊走の分子機構.	工藤翔二, 土屋了介, 金沢実, 大田健編	Annual Review 呼吸器 2004.	中外医学社	22-27 頁, 2004.
田中良哉.	細胞接着分子.	折茂肇編	骨粗鬆症―基礎・臨床研究の新しいパラダイム.	日本臨床社	125-130 頁, 2004.
田中良哉.	膠原病・リウマチ性疾患に起因する骨粗鬆症.	折茂肇編	骨粗鬆症―基礎・臨床研究の新しいパラダイム.	日本臨床社	677-682 頁, 2004.
田中良哉.	関節リウマチ.	名和田新編	ステロイド骨粗鬆症の治療マニュアル.	ライフサイエンス出版	38-45 頁, 2004.
田中良哉.	炎症反応(赤沈, CRP).	三森経世編	リウマチ膠原病診療チェックリスト.	文光堂	115-118 頁, 2004.
田中良哉.	白血球ー内皮細胞間接着の分子機構.	吉川敏一編	プロテアーゼインヒビター基礎編.	診断と治療社	198-203 頁, 2004.
田中良哉.	免疫疾患と T 細胞の役割.	永野允, 原田尚, 藤澤洌, 永野志朗編	内科診療 Q&A『免疫疾患』.	六法出版	46-49 頁, 2004.
田中良哉.	関節リウマチに対する抗 TNFα 抗体療法の有用性と問題点.	宮坂信之, 宮島篤編	サイトカイン – state of arts.	医歯薬出版	345-348 頁, 2004.
田中良哉.	多発性筋炎/皮膚筋炎.	河合眞一編	実地医家のためのステロイド薬の上手な使い方.	永井書店	75-81 頁, (2004).
田中良哉.	血管炎.	日本リウマチ学会編	リウマチ入門第 12 版.	日本リウマチ学会	451-483 頁, (2004).
田中良哉.	関節リウマチ（悪性関節リウマチを含む）.	高久文麿, 猿田享男, 北村惣一郎, 福井次夫編	家庭医学大百科.	法研	2907-2911 頁, (2004)
田中良哉.	CD20 抗体の自己免疫疾患の治療への応用.	岸本忠三編	免疫 2005.	中山書店	400-406 頁, (2004)
田中良哉, 藤井幸一.	炎症と修復.	浅香正博編	21 世紀の胃の炎症学.	メディカルレビュー社	301-310 頁, (2004)

Ⅳ. 研究成果の刊行物・別刷

Nucleosome-Specific Regulatory T Cells Engineered by Triple Gene Transfer Suppress a Systemic Autoimmune Disease[1]

Keishi Fujio,* Akiko Okamoto,* Hiroyuki Tahara,* Masaaki Abe,† Yi Jiang, † Toshio Kitamura,‡ Sachiko Hirose,† and Kazuhiko Yamamoto[2]*

The mechanisms of systemic autoimmune disease are poorly understood and available therapies often lead to immunosuppressive conditions. We describe here a new model of autoantigen-specific immunotherapy based on the sites of autoantigen presentation in systemic autoimmune disease. Nucleosomes are one of the well-characterized autoantigens. We found relative splenic localization of the stimulative capacity for nucleosome-specific T cells in (NZB × NZW)F_1 (NZB/W F_1) lupus-prone mice. Splenic dendritic cells (DCs) from NZB/W F_1 mice spontaneously stimulate nucleosome-specific T cells to a much greater degree than both DCs from normal mice and DCs from the lymph nodes of NZB/W F_1 mice. This leads to a strategy for the local delivery of therapeutic molecules using autoantigen-specific T cells. Nucleosome-specific regulatory T cells engineered by triple gene transfer (TCR-α, TCR-β, and CTLA4Ig) accumulated in the spleen and suppressed the related pathogenic autoantibody production. Nephritis was drastically suppressed without impairing the T cell-dependent humoral immune responses. Thus, autoantigen-specific regulatory T cells engineered by multiple gene transfer is a promising strategy for treating autoimmune diseases. ***The Journal of Immunology,*** **2004, 173: 2118–2125.**

Systemic autoimmune diseases have traditionally been treated using nonspecific immunosuppressive agents, but these agents often lead to opportunistic infections and an increased rate of malignancy. There remains the need to develop selective or specific therapies that target individual autoantigens. Several strategies have been developed as potential Ag-specific immunotherapies, such as using Ag-pulsed dendritic cells (DCs),[3] but the majority of these approaches will require further investigation (1, 2). A more detailed understanding of autoimmune diseases, including autoantigen presentation, is required for the development of reasonable immunotherapies.

Systemic lupus erythematosus (SLE) is a life-threatening autoimmune disease characterized by the production of a variety of autoantibodies (3). Anti-DNA Abs are thought to be one of the major pathogenic products of the autoimmune response (4–6). Datta and colleagues (7–9), as well as other groups (10, 11), have noted that nucleosomes could be a major immunogen for pathogenic autoantibody-inducing T cells in lupus-prone mice. Datta and coworkers (7–9) showed that the majority of pathogenic T_H clones specific for nucleosomes were capable of rapidly inducing anti-DNA autoantibody production, and that these clones were also able to induce nephritis when injected into young lupus-prone mice. Moreover, anti-nucleosome ELISAs have demonstrated better sensitivity, specificity, and diagnostic confidence with regard to human SLE than anti-DNA ELISAs. Anti-nucleosome ELISAs are also correlated with disease activity, as determined by the SLE Disease Activity Index (12, 13).

Although evidences have accumulated demonstrating the importance of nucleosomes as major pathogenic autoantigens, the cellular mechanisms for the immunological recognition of nucleosomes are poorly understood. Generalized hyperresponsiveness of B cells has been reported in both mice and human lupus (14, 15). However, these nonspecific immune disorders cannot provide a sufficient model of nuclear autoantigen-specific autoimmunity encountered in patients with lupus.

To better understand the mechanisms of autoantigen recognition, we first reconstituted nucleosome specificity by TCR gene transfer in $CD4^+$ T cells from (NZB × NZW)F_1 (NZB/W F_1) lupus model mice (3, 16). Using this model, we demonstrated an abnormal autoantigen presentation of splenic DCs. Among the lymphoid organs, this elevated autoantigen presentation of DCs was relatively localized in the spleen. We then developed a triple gene transfer system to generate autoantigen-specific regulatory cells. These regulatory cells preferentially accumulated in the spleen and suppressed the progression of the disease without obvious systemic immunosuppression.

Materials and Methods

Preparation of retroviral construct

Line 3A is a cell line from lupus-prone (SWR × NZB)F_1 (SNF1; I-$A^{d/q}$) that can recognize the immunodominant nucleosomal epitope (histone H4; aa 71–94) in the context of I-A^d (7, 8) and many other I-A molecules (8). Both TCR-α and -β cDNA fragments were synthesized using PCR based on the published sequences of line 3A (7, 8) and designated as AN3 TCR-α and -β. Vα13 and Vβ4 fragments identical to CDR1 and two sequences of line 3A were obtained from NZB splenic cDNA and an added CDR3 sequence by PCR. Jα41-Cα fragment and Jβ2.6-Cβ fragment were also obtained from NZB splenic cDNA and an added CDR3 sequence by PCR. Vα13-CDR3 fragment and CDR3-Jα41-Cα fragment were combined in a

*Department of Allergy and Rheumatology, Graduate School of Medicine, University of Tokyo, Tokyo, Japan; †Department of Pathology, Juntendo University School of Medicine, Tokyo, Japan; and ‡Division of Cellular Therapy, Advanced Clinical Research Center, Institute of Medical Science, University of Tokyo, Tokyo, Japan

Received for publication September 24, 2003. Accepted for publication May 12, 2004.

The costs of publication of this article were defrayed in part by the payment of page charges. This article must therefore be hereby marked *advertisement* in accordance with 18 U.S.C. Section 1734 solely to indicate this fact.

[1] This study was supported by grants from the Ministry of Health, Labor and Welfare and the Ministry of Education, Culture, Sports, Science and Technology of Japan.

[2] Address correspondence and reprint requests to Dr. Kazuhiko Yamamoto, Department of Allergy and Rheumatology, Graduate School of Medicine, University of Tokyo, 7-3-1 Hongo, Bunkyo-ku, Tokyo, 113-0033, Japan. E-mail address: yamamoto-tky@umin.ac.jp

[3] Abbreviations used in this paper: DC, dendritic cell; SLE, systemic lupus erythematosus; WPRE, woodchuck hepatitis virus posttranscriptional regulatory element; IRES, internal ribosomal entry site; LN, lymph node.

0022-1767/04/$02.00

subsequent "fusion" reaction in which the overlapping ends anneal, allowing the 3′ overlap of each strand to serve as a primer for the 3′ extension of the complementary strand. The resulting fusion product is amplified further by PCR. Vβ4-CDR3 fragment and CDR3-Jβ2.6-Cβ fragment were combined similarly. The full-length fragments were cloned into a pMXW retroviral vector to obtain pMXW-AN3α and pMXW-AN3β (Fig. 1*A*). pMXW is an improved vector generated by insertion of the woodchuck hepatitis virus posttranscriptional regulatory element (WPRE) (17, 18) between the *NotI* and *SalI* sites of pMX (19). WPRE enhances expression of transgenes delivered by retroviral vectors (18), and the expression efficiency of the pMXW vector is improved 1.5 times when WPRE is inserted, compared with the efficiency of the pMX vector. Murine CTLA4Ig cDNA was synthesized by PCR as described previously (20) and was then cloned into the pMX-IRES-GFP (21). Complementary DNAs for the TCR α- and β-chains were isolated from a cDNA library of DO11.10 TCR-transgenic splenocytes and were inserted into the retroviral vector pMX to generate pMX-DOTAE and pMX-DOTBE, respectively (22).

Mice

NZB/W F_1 and BALB/c mice were obtained from Japan SLC (Shizuoka, Japan). All animal experiments were conducted in accordance with the institutional and national guidelines.

Production of retroviral supernatants and retroviral transduction

Total splenocytes were isolated and cultured for 48 h in RPMI 1640 medium supplemented with 10% FCS, 2 mM L-glutamine, 100 U/ml penicillin, 100 μg/ml streptomycin, and 5×10^{-5} M 2-ME in the presence of Con A (10 μg/ml) and IL-2 (50 ng/ml) before the transduction. Retroviral supernatants were obtained by transfection of pMXW, pMXW-AN3α, pMXW-AN3β, pMX-IRES-GFP, pMX-CTLA4Ig-IRES-GFP, pMX-DOTAE, or pMX-DOTBE DNA into PLAT-E packaging cell lines (22, 23) with the use of the FuGENE 6 transfection reagent (Roche Diagnostic Systems, Somerville, NJ).

Falcon 24-well plates (BD Biosciences, San Jose, CA) were coated with the recombinant human fibronectin fragment CH296 (Retronectin; Takara, Otsu, Japan) according to the manufacturer's instructions. Before infection, virus-bound plates were prepared. The viral supernatant (500 μl) was preloaded onto each well of the CH296-coated plate, and the plate was spun at 2000 × *g* for 3 h at 32°C. The virus-coating procedure was repeated three times. Before infection, the viral supernatant was washed away and splenocytes prestimulated for 48 h were added to each well (1×10^6 cells/well). Cells were cultured for 36 h to allow infection to occur. To control the viral expression efficiency, we produced a viral supernatant (pMXW, pMXW-AN3α, pMXW-AN3β, pMX-IRES-GFP, and pMX-CTLA4Ig-IRES-GFP, simultaneously) and prechecked the uniformity of the infection efficiency before in vitro and in vivo experiments.

Cell purification

A $CD4^+$ T cell population was prepared by negative selection with MACS using anti-CD19 mAb, anti-CD11c, mAb, and anti-CD8a mAb. $CD11c^+$ DCs were prepared as previously described (24, 25). Briefly, spleen cells or lymph node cells were digested with collagenase type IV (Sigma-Aldrich, St. Louis, MO) and DNase I, and the $CD11c^+$ cells were selected twice by positive selection using MACS CD11c microbeads and magnetic separation columns. The purity (85% in average) was determined by visualization with anti-CD11c-biotin followed by streptavidin-PE. A $CD19^+$ B cell population was prepared by positive selection with MACS using anti-CD19 mAb. For CFSE labeling (Molecular Probes, Eugene, OR), cells were resuspended in PBS at 1×10^7/ml and incubated with CFSE at a final concentration of 5 mM for 30 min at 37°C, followed by two washes in PBS.

Nucleosome preparation

Pure nucleosomes were prepared as previously described (26). Briefly, frozen pure chicken erythrocytes were thawed and suspended in lysis buffer on ice (10 mM Tris-HCl, 10 mM NaCl, 5 mM $MgCl_2$, 0.5% Nonidet P-40, and 0.25 mM $PhMeSO_2F$, pH 7.5). The nuclei were recovered by centrifugation and the nuclear pellet was washed and digested with micrococcal nuclease. The nuclear pellet was lysed into 0.2 mM Na_2EDTA, and nuclear debris was removed by centrifugation. The soluble chromatin at $A_{260} \approx 100$ was dialyzed against 5 mM triethanolamine HCl, 60 mM NaCl, 1 mM Na_2EDTA (pH 7.5), and subsequently fractionated in the same buffer, usually in sucrose gradients. Gradients were fractionated and monitored at 280 nm, and the appropriate fractions were pooled.

Proliferation assay

At 24 h postinfection, purified $CD4^+$ T cells were cultured at 2×10^4cells/well, with 1×10^5 cells/well of irradiated $CD19^+$ B cells or 1×10^4 cells/well of irradiated $CD11c^+$ DCs in 96-well flat-bottom microtiter plates in volumes of 100 μl of complete medium with or without 1 μg/ml nucleosome or 0.3 μM chicken $OVA_{323-339}$ peptide. After 24 h of culture, the cells were pulse labeled with 1 μCi of [^{3}H]thymidine/well (NEN Life Science Products, Boston, MA) for 15 h and the [^{3}H]thymidine incorporation was determined. In some experiments, we calculated the ratio of (group A − cpm)/(group B − cpm) in each experiment and showed the average ratio of three to five experiments as "average ratio of (group A − cpm)/(group B − cpm) to clarify the reproducibility of the data.

Transfer experiments

The indicated number of cells suspended in PBS were i.v. injected into mice. For the transfer of gene-transduced cells, cell viability was always >97%, as detected by trypan blue exclusion.

ELISA

IgG anti-DNA Abs were quantified using ELISA plates coated with calf thymus DNA (Sigma-Aldrich, and the DNA-binding activities were expressed in units, referring to a standard curve obtained by serial dilutions of a standard serum pool from 7- to 9-mo-old NZB/W F_1 mice, containing 1000 U/ml. IgG antinucleosome Abs or IgG anti-histone Abs were quantified using ELISA plates coated with purified nucleosome or purified histone. Methods for detection of CTLA4Ig protein were described previously (27). Briefly, ELISA plates were coated with anti-mouse CTLA4 (BD PharMingen, San Diego, CA) overnight at 4°C, blocked with blocking solution, and then incubated sequentially for 1 h at 37°°C with serial dilutions of serum or culture supernatants followed by peroxidase-conjugated $F(ab')_2$ goat anti-mouse IgG2a (Accurate Antibodies, Westbury, NY) and ABTS substrate (Kirkegaard & Perry, Gaithersburg, MD). Serial dilutions of a known concentration of purified CTLA4Ig were used in each plate to establish a standard curve.

Histopathology

Organs were fixed in 4% paraformaldehyde, embedded in paraffin, and stained with periodic acid-Schiff solution. For three-color immunofluorescence staining, sections were incubated with biotinylated peanut agglutinin (Vector Laboratories, Burlingame, CA) and then with Cy5.5-conjugated streptavidin (Cortex Biochemicals, Irvine, CA). The sections were then stained with a rat Alexa488-labeled mAb to B220 and tetramethylrhodamine-conjugated mAbs to CD4 and CD8 (Vector Laboratories). To detect the deposition of immune complexes at glomeruli, we incubated sections with FITC-labeled goat Abs to mouse IgG or to C3 (ICN Pharmaceuticals, Costa Mesa, CA).

Statistical analysis

Statistical significance was determined using the unpaired Student's *t* test or the Mann-Whitney *U* test.

Results

Transduction of nucleosome-specific AN3 TCR confers specificity for the nucleosome and autoreactivity to DCs in NZB/W F_1 $CD4^+$ T cells

We previously reported successful TCR gene transfer and reconstitution of the Ag specificity to OVA in BALB/c $CD4^+$ T cells (27). In the present study, we transferred nucleosome-specific TCR genes (AN3α and β) into NZB/W F_1 splenocytes. To improve the expression of the introduced genes, we generated a Moloney-based retroviral vector, pMXW, by insertion of the woodchuck fragment (17, 18) into pMX (19). We selected the TCR of line 3A from lupus-prone SNF1 mice. A hybridoma transfected with this TCR did not exhibit any significant response to either $H\text{-}2^d$ or $H\text{-}2^z$ APCs (28). Each TCR gene was inserted into pMXW, and the resulting retrovirus vectors (pMXW-AN3α and pMXW-AN3β) were used for the gene transfer (Fig. 1*A*).

Retroviral infection of the AN3 TCR genes into NZB/W F_1 splenocytes induced a 40–45% increase in the $V\beta4^+$ population in $CD4^+$ T cells compared with mock-infected splenocytes (Fig. 1*B*). The calculated efficiency of the Vβ4 introduction into the

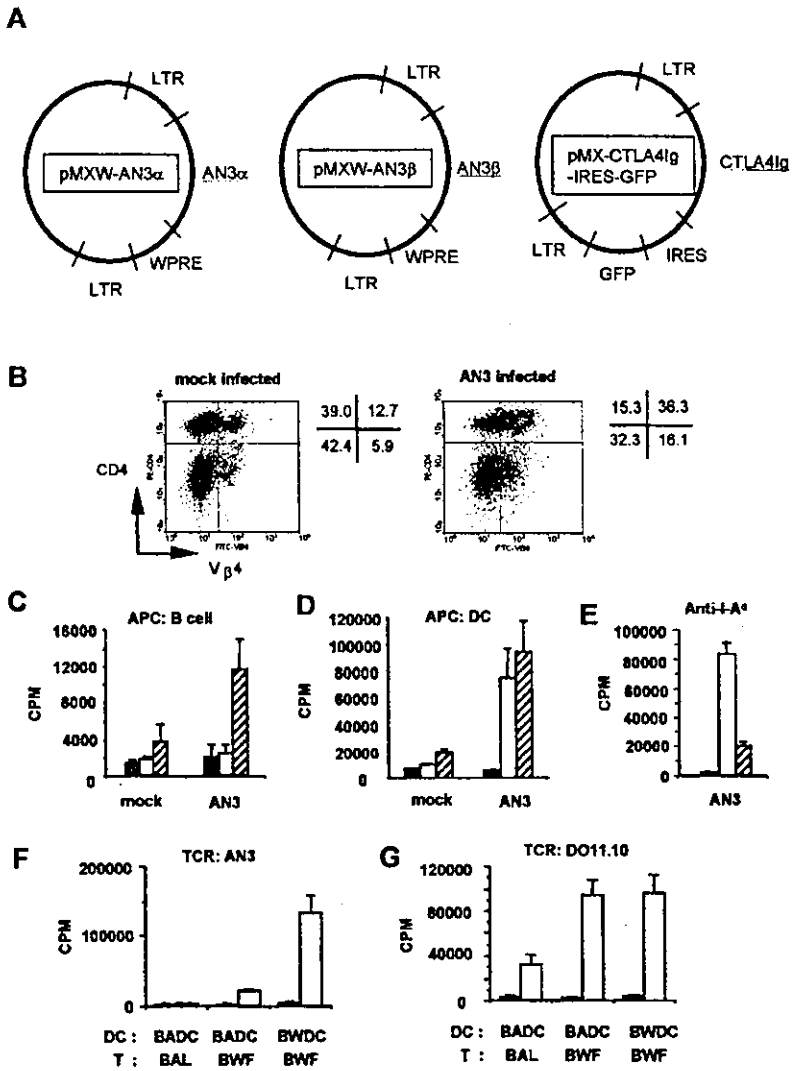

FIGURE 1. Retroviral transfer of AN3 TCR reconstituted the specificity for nucleosomes on NZB/W F_1 $CD4^+$ T cells. Reconstituted T cells showed autoreactivity to splenic DCs. *A*, Schematic representation of the pMXW retrovirus construct expressing the cDNA for the AN3 TCRα or TCRβ chain. LTR, long terminal repeat. *B*, Anti-CD4 and anti-Vβ4 staining of pMXW (mock) or AN3 TCR-transduced NZB/W F_1 splenocytes. Results of a representative experiment are shown. *C*, Proliferation of AN3-transduced and mock-transduced $CD4^+$ T cells to B cells with nucleosomes. ■, T cells alone; □, T + B; ▨, T + B + nucleosomes (1 μg/ml). *D*, Proliferation of AN3-transduced and mock-transduced $CD4^+$ T cells to $CD11c^+$ DCs with nucleosomes. ■, T cells alone; □, T + DCs; ▨, T + DCs + nucleosomes (1 μg/ml). *E*, Blockade of AN3-transduced $CD4^+$ T cell proliferation to NZB/W F_1 $CD11c^+$ DCs by an anti-I-A^d Ab, K24-199. ■, T cells alone; □, T + DCs; ▨, T + DCs + anti-I-A^d Ab. *F*, Proliferative response of AN3- or mock-transduced $CD4^+$ T cells from BALB/c (BAL) or NZB/W F_1 (BWF) (■, mock-transduced cells; □, AN3-transduced cells) with BALB/c $CD11c^+$ DCs (BADC) or NZB/W F_1 $CD11c^+$ DCs (BWDC). *G*, Proliferative response of DO11.10- and mock-transduced $CD4^+$ T cells from BALB/c (BAL) or NZB/W F_1 (BWF) (■, mock-transduced cells; □, DO11.10-transduced cells with 0.3 μM $OVA_{323-339}$) with BALB/c $CD11c^+$ DCs (BADC) or NZB/W F_1 $CD11c^+$ DCs (BWDC). Data shown are representative of more than three independent experiments with similar results.

$CD4^+V\beta4^-$ population was 50–60%. The lack of anti-Vα13 or anti-clonotypic Abs prevented direct visualization of AN3 TCR surface expression. However, based on the transduction of other TCR pairs (i.e., OVA-specific DO11.10 TCR detected by a clonotypic Ab KJ1-26; and AV8/BV7, detectable by anti-Vα8 and anti-Vβ7 Abs; data not shown), we speculate that Vα chain expression is approximately equal to that of the Vβ chain. Thus, the proportion of clonotypic AN3 TCR-expressing cells was estimated to be 25–36% in $CD4^+$ T cells. These cells were referred to as BWF.AN3, and the mock-infected $CD4^+$ T cells were referred to as BWF.mock.

We investigated the specific reactivity to the nucleosomes of BWF.AN3 in the presence of NZB/W F_1 B cells and DCs. Although BWF.mock cells showed minimal proliferation in the presence of B cells and the nucleosomes, BWF.AN3 showed strong proliferation in the presence of B cells and the nucleosomes, but not in the presence of B cells alone (Fig. 1*C*). The average ratio of (BWF.AN3 - cpm)/(BWF.mock − cpm) was 1.13 ± 0.12 and that of (BWF.AN3 with nucleosome (nuc) − cpm)/(BWF.mock with nuc − cpm) was 3.12 ± 0.51 in three experiments ($p < 0.005$). These results demonstrate that the introduction of AN3 TCR reconstitutes the specificity for the nucleosome on $CD4^+$ T cells. Furthermore, BWF.AN3 showed proliferation in the presence of splenic DCs without nucleosome (Fig. 1*D*). The average ratio of (BWF.AN3 − cpm)/(BWF.mock − cpm) was 6.97 ± 1.63 in five experiments ($p < 0.001$). Consistent with previous report that $CD4^+$ T cells of lupus-prone mice responded to nucleosome ex vivo (7), BWF.mock showed relatively weak proliferation in the presence of splenic DCs and nucleosome. The average ratio of (BWF.mock with nuc − cpm)/(BWF.mock − cpm) was 2.21 ± 0.73 in five experiments ($p < 0.05$). Despite these endogenous responses of BWF.mock to nucleosome, BWF.AN3 showed stronger proliferation compared with BWF.mock in the presence of splenic DCs with the nucleosomes. The average ratio of (BWF.AN3 with nuc − cpm)/(BWF.mock with nuc − cpm) was 4.01 ± 2.18 in five experiments ($p < 0.05$).

AN3α-infected or β-infected cells failed to respond to the DCs (data not shown), and the autoreactive response was blocked by anti-I-A^d Ab (Fig. 1*E*). Thus, this autoreactivity of BWF.AN3 to splenic DCs suggests that NZB/W F_1 splenic DCs spontaneously present a considerable amount of nucleosomal epitopes.

The nucleosome-specific response of NZB/W F_1 mice consisted of general T cell hyperreactivity and Ag-specific hyperpresentation of splenic DCs

To investigate the relative contribution of either T cells or splenic DCs to the autoreactive response, we also transduced the AN3 TCR into BALB/c $CD4^+$ T cells and these cells were referred to

as BAL.AN3. Although BAL.AN3 showed no proliferative response to BALB/c splenic DCs, BWF.AN3 showed a moderate proliferative response to BALB/c splenic DCs (Fig. 1*F*). These results suggest that the BWF1 T cell hyperreactivitiy enables BWF.AN3 to recognize small amounts of nucleosomal epitope presented on BALB/c splenic DCs, but these small amounts are ignored by BAL.AN3. As expected, BWF.AN3 strongly responded to BWF1 splenic DCs. Proliferative response of BWF.AN3 in the presence of BALB/c splenic DCs amounted to ~14–18% of that to BWF1 splenic DCs, indicating that the abnormal presentation of splenic DCs may contribute more to the autoreactive response than does T cell hyperreactivity.

To determine the general Ag recognition and reactivity of NZB/W F_1 mice, we examined the proliferation of T cells transduced with OVA-specific TCR (DO11.10). Fifty to 60% of the total $CD4^+$ T cells expressed the introduced DO11.10 TCR, as determined by the anti-clonotypic Ab KJ1-26. DO11.10-transduced BWF1 T cells cultured with DCs plus $OVA_{323-339}$ peptide exhibited stronger proliferation than BALB/c T cells, again suggesting that BWF1 T cells possess general hyperreactivity. In contrast, the OVA peptide-presentation (Fig. 1*G*) and the whole OVA presentation (data not shown) of NZB/W F_1 splenic DCs appeared to be quite similar to that of BALB/c splenic DCs. Thus, the hyperpresentation of DCs seems to be restricted to a certain Ag.

Nucleosome-specific T cells interacted with the autoantigen in the spleen

DCs in every type of lymphoid tissue may present nucleosomal epitopes, because nucleosomal Ags are available in every organ. To investigate this possibility, we fluorescently labeled either BWF.mock or BWF.AN3 T cells in vitro with CFSE and injected them into NZB/W F_1 mice. Two days after the transfer, T cells from the spleen and those from the peripheral lymph nodes (LNs) were harvested and analyzed. BWF.mock isolated from the spleen exhibited a convergent strong fluorescence peak, indicating that these cells had not proliferated extensively. In contrast, BWF.AN3 isolated from the spleen exhibited several weaker fluorescence peaks. Moreover, AN3 $CD4^+$ T cells underwent multiple divisions over a 5-day period of the experiment, and mock $CD4^+$ T cells underwent a very slight progression of cell division (Fig. 2*A*). These findings suggested that BWF.AN3 encountered the nucleosomal epitope in the spleen. It was of note that both CFSE-labeled BWF.mock and BWF.AN3 isolated from the peripheral LNs exhibited a strong convergent fluorescence peak, suggesting that BWF.AN3 encountered the nucleosomal epitope less frequently in the LNs.

A comparison of the stimulative capacity for BWF.AN3 also suggested that splenic DCs presented more nucleosomal epitope than DCs from the peripheral LNs (Fig. 2*B*). The average ratio of (BWsplDC − cpm)/(BWLNDC − cpm) was 2.79 ± 0.44 in three experiments ($p < 0.005$). These results showed that nucleosome-specific T cells are stimulated predominantly in the spleen.

Effect of CTLA4Ig transfer on the nucleosomal response

We next tried to generate nucleosome-specific regulatory cells by introducing an immunosuppressive molecule, CTLA4Ig, as the third gene in BWF.AN3 T cells. Long-term administration of CTLA4Ig to NZB/W F_1 mice has been shown to prevent disease onset for a period of months (29).

We constructed a pMX-CTLA4Ig-IRES-GFP vector (Fig. 1*A*). We then performed a triple gene transfer of the AN3$\alpha\beta$ and CTLA4Ig genes to investigate the effect on CTLA4Ig expression. The experimental groups consisted of $CD4^+$ T cells transduced with either AN3 + CTLA4Ig-IRES-GFP(CTLA4Ig), AN3 + IRES-GFP(IG), pMXW(mock) + CTLA4Ig, or mock + IG. The average expression efficiency from several different sets of infection was 45.2% for Vβ4 and 47.3% for GFP in $CD4^+$ cells (Fig. 3*A*). The average expression efficiency is expected to be 45% for the AN3α gene, and the average percentage of GFP^+AN3^+ cells expressing all three gene products in $CD4^+$ T cells was estimated to be ~10% (0.45 × 0.45 × 0.45). As shown in Fig. 3*B*, the CTLA4Ig secreted from T cells blocked the proliferation of the endogenous T cell population to the nucleosome to a moderate degree. The average ratio of (mock + CTLA4Ig with nuc − cpm)/(mock + IG with nuc − cpm) was 0.40 ± 0.07 in three experiments ($p < 0.005$). But the T cell stimulation mediated by AN3 TCR was not blocked by CTLA4Ig. The average ratio of (AN3 + IG − cpm)/(mock + IG − cpm) was 7.85 ± 1.07 and that of (AN3 + CTLA4Ig − cpm)/(mock + IG − cpm) was 7.18 ± 0.96 in three experiments. The AN3 + CTLA4Ig transduced cells showed the increase of CTLA4Ig secretion on T cell activation in the presence of DCs (Fig. 3*C*).

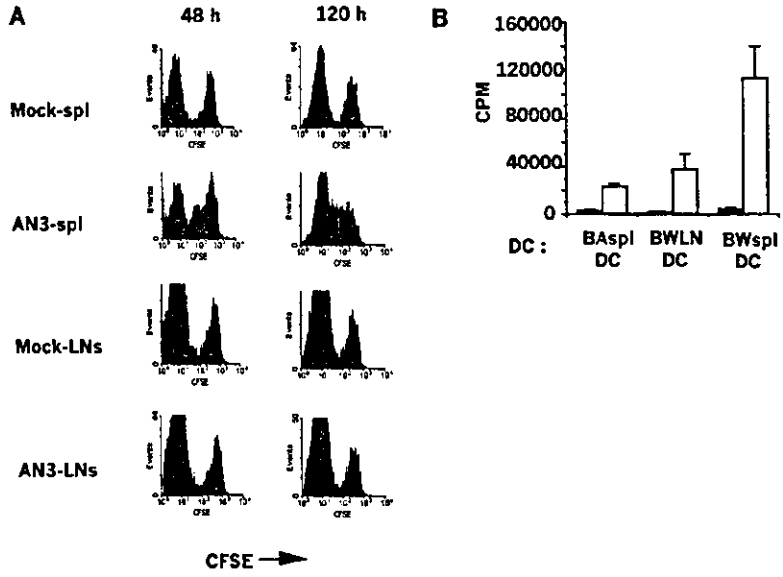

FIGURE 2. Nucleosome-specific T cells were stimulated more strongly in the spleen than in the LNs. *A*, CFSE-labeled BWF_1.mock T cells or BWF.AN3 T cells were transferred i.v. into 10-wk-old NZB/W F_1 mice. Two and 5 days later, splenocytes or peripheral LNs (cervical, inguinal, and mesenteric) from recipient mice were examined for $CFSE^+V\beta4^+$-gated cells. *B*, Proliferation of AN3- or mock-transduced T cells to $CD11c^+$ DCs from the spleen or LNs. $CD11c^+$ DCs from NZB/W F_1 spleens (BWsplDC), from NZB/W F_1 LNs (BWLNDC) and from BALB/c spleens (BAsplDC). Data shown are representative of three independent experiments with similar results.

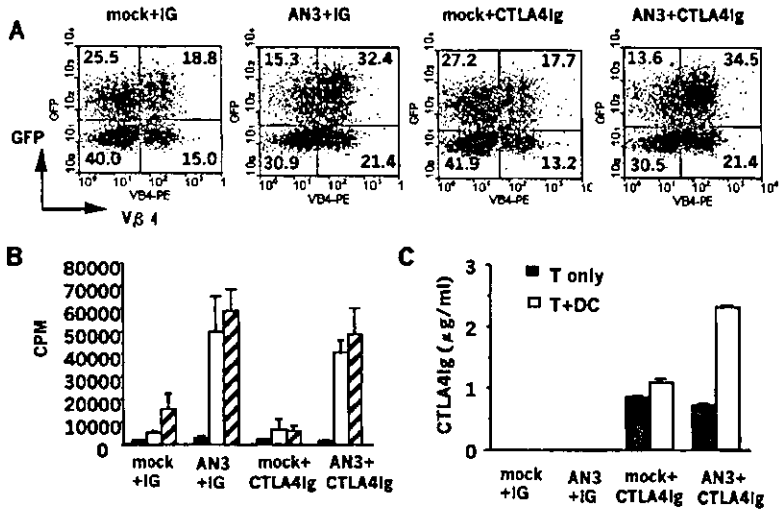

FIGURE 3. Effect of CTLA4Ig gene transfer on the T cell proliferation to nucleosomes. *A*, Expression analysis of GFP and Vβ4 in gene-transduced cells gated for CD4. The transduction efficiency was ~45% for a single gene in each group. *B*, Suppressive effect of CTLA4Ig transduction on T cell activation to nucleosomes. ■, T cells alone; □, T + DCs; ▨, T + DCs + nucleosome. *C*, CTLA4Ig production of T cells with or without DCs. Each culture supernatant was harvested after 24 h of culture. Data shown are representative of three independent experiments with similar results.

Nucleosome-specific regulatory cells suppressed autoimmune disease

We transferred cell suspensions containing 1×10^6 cells of $CD4^+$ T cells, calculatedly expressing either AN3 + CTLA4Ig, AN3 + IG, mock + CTLA4Ig, or mock + IG into 10-wk-old NZB/W F_1 mice.

The autoantibodies usually found in NZB/W F_1 mice were measured in the sera from the different groups. The elevations of anti-dsDNA and anti-histone Abs were suppressed in AN3 + CTLA4Ig-injected mice at 22 wk of age (Fig. 4*A*). AN3 + CTLA4Ig-injected mice showed the lowest average titer of anti-nucleosome Ab, but the titer in this group was not significantly different from those in the controls. This inefficient suppression may be due to the fact that autoimmunity to the nucleosome is the driving reaction and that this reaction is stronger than the subsequent response.

The mice were monitored biweekly for proteinuria. By week 22, control mice that had received PBS, mock + IG, AN3 + IG, or

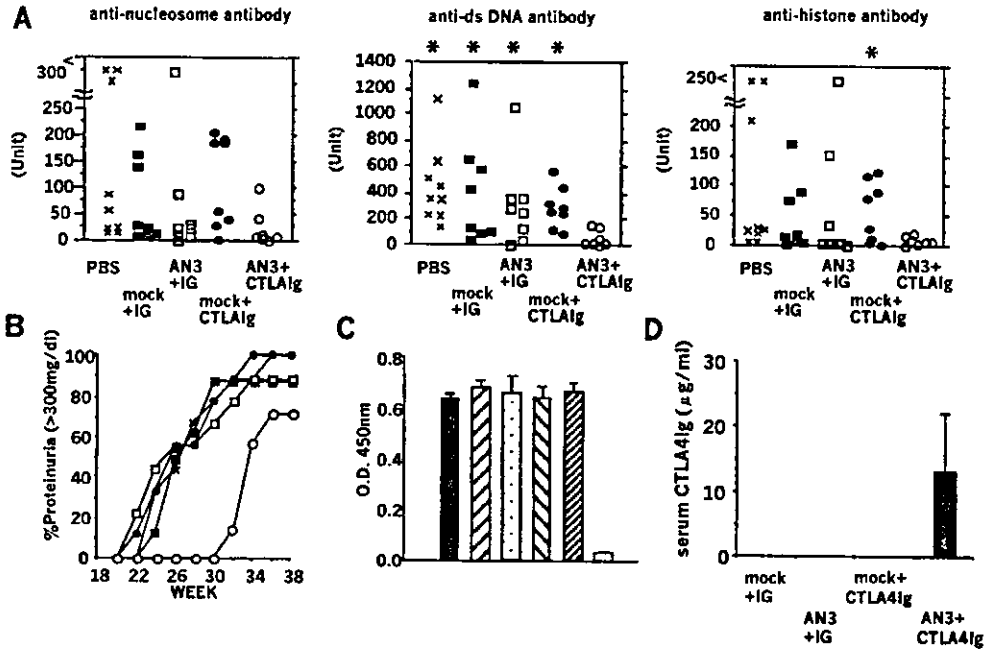

FIGURE 4. Effect of adoptively transferred engineered cells on disease progression. *A*, Suppression of autoantibody production. The elevation of serum anti-nucleosome, anti-dsDNA, and anti-histone Abs, measured by ELISA, was suppressed in AN3 + CTLA4Ig-injected mice at 22 wk. Statistically significant differences between AN3 + CTLA4Ig and control groups are denoted by asterisks ($p < 0.05$); $n = 7$ for AN3 + CTLA4Ig, and $n = 8$ for each control group. *B*, Cumulative percentage of mice in each group that developed severe proteinuria (>300 mg/dl). AN3 + CTLA4Ig showed suppressed progression of proteinuria compared with the control groups. x, PBS; ■, mock + IG; □, AN3 + IG; ●, mock + CTLA4Ig; ○, AN3 + CTLA4Ig. AN3 + CTLA4Ig vs the controls at 30 wk was significant ($p < 0.05$). *C*, A T cell-dependent humoral immune response to active immunization of OVA. Mice transferred with the engineered T cells at 10 wk of age were immunized with OVA in the footpad at 14 wk of age. Anti-OVA IgG Ab titer was measured at 17 wk of age. ■, PBS; ▨, mock + IG; ▩, AN3 + IG; ▧, mock + CTLA4Ig; ▨, AN3 + CTLA4Ig; □, no immunization. $n = 6$/group. *D*, Measurement of serum CTLA4Ig protein in the experimental groups with ELISA. Only AN3 + CTLA4Ig-transferred mice showed detectable, but low concentration of CTLA4Ig protein.

mock + CTLA4Ig started developing severe nephritis, as diagnosed by persistent proteinuria of >300 mg/dl. By 30 wk of age, 89% of the PBS control group, 88% of the mock + IG group, 63% of the AN3 + IG group, and 75% of the mock + CTLA4Ig group of mice had developed severe proteinuria, whereas none of the AN3 + CTLA4Ig mice showed excess proteinuria (Fig. 4*B*). However, the AN3 + CTLA4Ig-transferred mice started to develop severe proteinuria at 32 wk of age. Splenomegaly and an increase in the CD4:CD8 ratio, usually observed in aged NZB/W F_1 mice, were suppressed in AN3 + CTLA4Ig-injected mice (data not shown).

The kidneys from the controls and AN3 + CTLA4Ig-injected mice were examined at 30 wk of age (Fig. 5, *A–F*). Control mice had severe glomerulonephritis with mesangial proliferation and thickening of the capillary walls with marked deposition of IgG and complement. AN3 + CTLA4Ig-injected mice had mild glomerular lesions and deposition of IgG and complement was only restricted to the mesangial area. Although mock + CTLA4Ig-transferred mice showed formation of a number of large follicles with T cell invasion in the spleen, AN3 + CTLA4Ig-transferred mice showed only a limited number of small follicles (Fig. 5, *G* and *H*).

AN3 + CTLA4Ig-treated mice exhibited the normal humoral immune response upon active immunization

We next examined the T cell-dependent humoral immune response to active immunization of OVA. Mice transferred with the engineered T cells at 10 wk of age were immunized with OVA (100 μg) with CFA at 14 wk of age and boosted with OVA with IFA at 16 wk of age. The level of anti-OVA IgG Ab titer from 17-wk-old mice treated with AN3 + CTLA4Ig was not significantly different from those of the control mice (Fig. 4*C*). AN3 + CTLA4Ig transferred mice, but not other experimental groups, had low but detectable levels of serum CTLA4Ig (13.4 ± 10.1 μg/ml) (Fig. 4*D*), findings consistent with in vitro data shown in Fig. 3*C*. These results suggest that the engineered regulatory cells are sufficient to suppress autoimmune disease. However, they are not enough to induce general immunosuppression, because of the low serum level of CTLA4Ig in AN3 + CTLA4Ig-transferred mice.

Discussion

In this study, we demonstrated T cell hyperresponsiveness and the possibility of nucleosomal hyperpresentation of splenic DCs in NZB/W F_1 mice. In addition to the involvement of T cell hyperresponsiveness in Ab-mediated autoimmune disease (30), our results strongly suggest that the autoantigen hyperpresentation of DCs could contribute to the initiation and propagation of the response to the autoantigen, thereby resulting in florid autoimmune disease. This observation is consistent with those from previous reports indicating that mice with T cell hyperresponsiveness develop only a mild form of lupus-like symptoms (31, 32). Since hyperpresentation was not observed in the case of an exogenous Ag, OVA (peptides and whole protein), it is possible that the autoantigen hyperpresentation of splenic DCs was not due to the general hyperpresentation, e.g., excessive costimulatory signals, but rather to some Ag-restricted phenomenon. These features may be nucleosome specific, as reported in a previous study demonstrating that lupus-prone B6.NZMc1 mice showed nucleosome reactivity of T cells without generalized immunological deficits of B cells and T cells (33).

Although disease-related increases in the number of splenic DCs and chemokine production by myeloid DCs have been reported (34), these abnormalities have been observed in aged lupus-prone mice. Our finding of autoantigen hyperpresentation in the splenic DCs of young mice (10 wk) suggests the significance of the autoantigen hyperpresentation of splenic DCs in the pathogenesis of lupus.

Autoreactive response of nucleosome-specific T cells was much more prominent in the spleen than in the LNs. Although the mixed I-A haplotype of Aβz/Aαd molecules in NZB/W F_1 mice (35) may be associated with autoreactive response of AN3 infectant, the absence of the autoreactivity to B cells and DCs from peripheral LNs strongly suggests the requirement of an autoantigen for the autoreactivity. Differences between the splenic DCs and DCs from other peripheral lymphoid organs have been reported, including differences in the expression of chemokines (36) and chemokine receptors (37). Otherwise, localization of tissue-specific autoantigen among secondary lymphoid organs may be one explanation. For example, although DCs in the gastric LNs are known to exhibit constitutive presentation of gastric parietal cell-specific H^+/K^+-ATPase, peripheral or mesenteric DCs do not (38). Thus, the spleen could be one of the main sources of nucleosomes. Increased frequency of splenic apoptosis in SNF1 lupus mice has also been reported (23). Moreover, an insufficient complement system may allow apoptotic waste material to accumulate in the spleen (i.e., the "waste disposal" hypothesis) (39).

In our study, the therapeutic effect with minimal systemic immunosuppression was archived by the use of nucleosome-specific T cells secreting CTLA4Ig. Although elevation of CTLA4Ig protein was detected in the serum of AN3 + CTLA4Ig mice, the

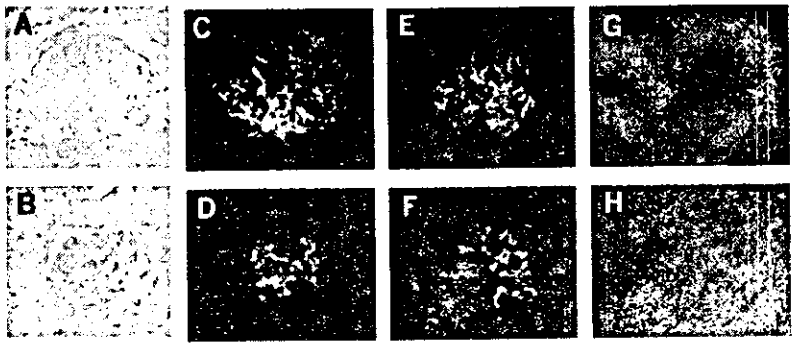

FIGURE 5. Histological examination from the AN3 + CTLA4Ig-treated mice compared with control mice. Sections of kidney from mock + IG-injected mice (*A*, *C*, and *E*) and AN3 + CTLA4Ig-injected mice (*B*, *D*, and *F*) subjected to staining with periodic-acid-Schiff solution (*A* and *B*) or to immunofluorescence staining with anti-IgG (*C* and *D*) or anti-C3 (*E* and *F*). Immunofluorescence staining of sections from the spleen, from mock + CTLA4Ig-injected mice (*G*), and from AN3 + CTLA4Ig-injected mice (*H*) with Abs to B220 (green), CD4 and CD8 (red), and with peanut agglutinin (blue). A section from one representative mouse from the indicated group is shown.

average concentration of CTLA4Ig in AN3 + CTLA4Ig mice is less than one-tenth of the level of previous systemic CTLA4Ig treatment with 5×10^8 PFU of adenovirus (27). Although the systemic adenoviral-CTLA4Ig (5×10^8 PFU) treatment exhibited a therapeutic effect equivalent to that of our experiment, the systemic treatment was accompanied with generalized immunosuppression. Since autoantigen-specific CTLA4Ig-secreting T cells showed normal Ab production on active immunization, this treatment may be superior to systemic CTLA4Ig administration. However, a systemic effect of a very low level of CTLA4Ig cannot be excluded and should be investigated further.

It is not surprising that 10^6 AN3 + mock cells did not aggravate the disease, since as many as 4×10^7 original L3A clone cells were needed to accelerate lupus nephritis in young lupus-prone mice (40). Thus, a relatively small amount of Ag-specific and potentially pathogenic T cells could be used for the immunotherapy. Foxp3, a member of the transcription factor family, has been identified as a key molecule for the development of $CD4^+CD25^+$ regulatory T cells (41). Retroviral transfer of Foxp3 confers regulatory function on $CD4^+CD25^-$ T cells. The introduction of such regulatory molecules with TCR could possibly generate Ag-specific regulatory T cells.

In a preliminary analysis of the persistence of the transferred genes in the spleen and LNs from 30-wk-old mice with RT-PCR, expression of AN3α gene was detected in the spleens from two of two AN3 + IG^- and AN3 + CTLA4Ig^--injected mice (data not shown). These results may suggest the persistence of introduced genes at 20 wk after the transfer in the spleen.

Although several models of adoptive cell gene therapy have been reported using T cell hybridomas or lines (42, 43), our method has the advantage of using autologous lymphocytes for gene recipients. However, TCR-transduced recipient T cells could gain heterodimeric TCR consisting of endogenous and exogenous chains. If such an unexpected TCR recognizes a certain unrelated self-derived molecule, the transduced T cells may be harmful. We did not observe evident autoreactivity in single AN3α or AN3β genes transferred into $CD4^+$ T cells (data not shown), and the renal disease of AN3 TCR-transferred mice was not accelerated (Fig. 5*B*). There was a recent report of tumor rejection mediated by retrovirally reconstituted Ag-specific T cells without any significant autoimmune pathology (44, 45). However, the possibility of developing autoimmunity should be carefully investigated further in application of TCR gene transfer.

In the present study, the efficacy of triple gene transfer in peripheral T cells was demonstrated for the first time. Although several improvements of the present method are still necessary, these findings suggest that the direct engineering of Ag-specific functional cells with multiple gene transfer is a powerful technique for the development of future Ag-specific therapies.

Acknowledgments

We are grateful to Kazumi Abe and Shiho Ohta for their excellent technical assistance.

References

1. Zitvogel, L., J. I. Mayordomo, T. Tjandrawan, A. B. DeLeo, M. R. Clarke, M. T. Lotze, and W. J. Storkus. 1996. Therapy of murine tumors with tumor peptide-pulsed dendritic cells: dependence on T cells, B7 costimulation, and T helper cell 1-associated cytokines. *J. Exp. Med. 183:87.*
2. Nestle, F. O., S. Alijagic, M. Gilliet, Y. Sun, S. Grabbe, R. Dummer, G. Burg, and D. Schadendorf. 1998. Vaccination of melanoma patients with peptide- or tumor lysate-pulsed dendritic cells. *Nat. Med. 4:328.*
3. Steinberg, A. D., M. F. Gourley, D. M. Klinman, G. C. Tsokos, D. E. Scott, and A. M. Krieg. 1991. NIH conference: systemic lupus erythematosus. *Ann. Intern. Med. 115:548.*
4. Lambert, P. H., and F. J. Dixon. 1968. Pathogenesis of the glomerulonephritis of NZB/W mice. *J. Exp. Med. 127:507.*
5. Dixon, F. J., M. B. Oldstone, and G. Tonietti. 1971. Pathogenesis of immune complex glomerulonephritis of New Zealand mice. *J. Exp. Med. 134(Suppl.):65s.*
6. Winfield, J. B., I. Faiferman, and D. Koffler. 1977. Avidity of anti-DNA antibodies in serum and IgG glomerular eluates from patients with systemic lupus erythematosus: association of high avidity antinative DNA antibody with glomerulonephritis. *J. Clin. Invest. 59:90.*
7. Mohan, C., S. Adams, V. Stanik, and S. K. Datta. 1993. Nucleosome: a major immunogen for pathogenic autoantibody-inducing T cells of lupus. *J. Exp. Med. 177:1367.*
8. Kaliyaperumal, A., C. Mohan, W. Wu, and S. K. Datta. 1996. Nucleosomal peptide epitopes for nephritis-inducing T helper cells of murine lupus. *J. Exp. Med. 183:2459.*
9. Lu, L., A. Kaliyaperumal, D. T. Boumpas, and S. K. Datta. 1999. Major peptide autoepitopes for nucleosome-specific T cells of human lupus. *J. Clin. Invest. 104:345.*
10. Burlingame, R. W., R. L. Rubin, R. S. Balderas, and A. N. Theofilopoulos. 1993. Genesis and evolution of antichromatin autoantibodies in murine lupus implicates T-dependent immunization with self antigen. *J. Clin. Invest. 91:1687.*
11. Burlingame, R. W., M. L. Boey, G. Starkebaum, and R. L. Rubin. 1994. The central role of chromatin in autoimmune responses to histones and DNA in systemic lupus erythematosus. *J. Clin. Invest. 94:184.*
12. Amoura, Z., S. Koutouzov, H. Chabre, P. Cacoub, I. Amoura, L. Musset, J. F. Bach, and J. C. Piette. 2000. Presence of antinucleosome autoantibodies in a restricted set of connective tissue diseases: antinucleosome antibodies of the IgG3 subclass are markers of renal pathogenicity in systemic lupus erythematosus. *Arthritis Rheum. 43:76.*
13. Bruns, A., S. Blass, G. Hausdorf, G. R. Burmester, and F. Hiepe. 2000. Nucleosomes are major T and B cell autoantigens in systemic lupus erythematosus. *Arthritis Rheum. 43:2307.*
14. Desai-Mehta, A., L. Lu, R. Ramsey-Goldman, and S. K. Datta. 1996. Hyperexpression of CD40 ligand by B and T cells in human lupus and its role in pathogenic autoantibody production. *J. Clin. Invest. 97:2063.*
15. Liossis, S. N., B. Kovacs, G. Dennis, G. M. Kammer, and G. C. Tsokos. 1996. B cells from patients with systemic lupus erythematosus display abnormal antigen receptor-mediated early signal transduction events. *J. Clin. Invest. 98:2549.*
16. Wofsy, D., and W. E. Seaman. 1985. Successful treatment of autoimmunity in NZB/NZW F_1 mice with monoclonal antibody to L3T4. *J. Exp. Med. 161:378.*
17. Donello, J. E., J. E. Loeb, and T. J. Hope. 1998. Woodchuck hepatitis virus contains a tripartite posttranscriptional regulatory element. *J. Virol. 72:5085.*
18. Zufferey, R., J. E. Donello, D. Trono, and T. J. Hope. 1999. Woodchuck hepatitis virus posttranscriptional regulatory element enhances expression of transgenes delivered by retroviral vectors. *J. Virol. 73:2886.*
19. Kitamura, T., M. Onishi, S. Kinoshita, A. Shibuya, A. Miyajima, and G. P. Nolan. 1995. Efficient screening of retroviral cDNA expression libraries. *Proc. Natl. Acad. Sci. USA 92:9146.*
20. Wallace, P. M., J. S. Johnson, J. F. MacMaster, K. A. Kennedy, P. Gladstone, and P. S. Linsley. 1994. CTLA4Ig treatment ameliorates the lethality of murine graft-versus-host disease across major histocompatibility complex barriers. *Transplantation 58:602.*
21. Kawashima, T., K. Hirose, T. Satoh, A. Kaneko, Y. Ikeda, Y. Kajiro, T. Nosaka, and T. Kitamura. 2000. MgcRacGAP is involved in the control of growth and differentiation of hematopoietic cells. *Blood 96:2116.*
22. Fujio, K., Y. Misaki, K. Setoguchi, S. Morita, K. Kawahata, I. Kato, T. Nosaka, K. Yamamoto, and T. Kitamura. 2000. Functional reconstitution of class II MHC-restricted T cell immunity mediated by retroviral transfer of the $\alpha\beta$ TCR complex. *J. Immunol. 165:528.*
23. Morita, S., T. Kojima, and T. Kitamura. 2000. Plat-E: an efficient and stable system for transient packaging of retroviruses. *Gene Ther. 7:1063.*
24. Kalled, S. L., A. H. Cutler, and L. C. Burkly. 2001. Apoptosis and altered dendritic cell homeostasis in lupus nephritis are limited by anti-CD154 treatment. *J. Immunol. 167:1740.*
25. Akbari, O., R. H. DeKruyff, and D. T. Umetsu. 2001. Pulmonary dendritic cells producing IL-10 mediate tolerance induced by respiratory exposure to antigen. *Nat. Immunol. 2:725.*
26. Bates, D. L., P. J. Butler, E. C. Pearson, and J. O. Thomas. 1981. Stability of the higher-order structure of chicken-erythrocyte chromatin in solution. *Eur. J. Biochem.119:469*
27. Mihara, M., I. Tan, Y. Chuzhin, B. Reddy, L. Budhai, A. Holzer, Y. Gu, and A. Davidson. 2000. CTLA4Ig inhibits T cell-dependent B-cell maturation in murine systemic lupus erythematosus. *J. Clin. Invest. 106:91.*
28. Shi, Y., A. Kaliyaperumal, L. Lu, S. Southwood, A. Sette, M. A. Michaels, and S. K. Datta. 1998. Promiscuous presentation and recognition of nucleosomal autoepitopes in lupus: role of autoimmune T cell receptor α chain. *J. Exp. Med. 187:367.*
29. Finck, B. K., P. S. Linsley, and D. Wofsy. 1994. Treatment of murine lupus with CTLA4Ig. *Science 265:1225.*
30. Vratsanos, G. S., S. Jung, Y. M. Park, and J. Craft. 2001. $CD4^+$ T cells from lupus-prone mice are hyperresponsive to T cell receptor engagement with low and high affinity peptide antigens: a model to explain spontaneous T cell activation in lupus. *J. Exp. Med. 193:329.*
31. Murga, M., O. Fernandez-Capetillo, S. J. Field, B. Moreno, L. R. Borlado, Y. Fujiwara, D. Balomenos, A. Vicario, A. C. Carrera, S. H. Orkin, M. E. Greenberg, and A. M. Zubiaga. 2001. Mutation of E2F2 in mice causes enhanced T lymphocyte proliferation, leading to the development of autoimmunity. *Immunity 15:959.*

32. Mohan, C., Y. Yu, L. Morel, P. Yang, and E. K. Wakeland. 1999. Genetic dissection of Sle pathogenesis: Sle3 on murine chromosome 7 impacts T cell activation, differentiation, and cell death. *J. Immunol. 162:6492.*
33. Mohan, C., E. Alas, L. Morel, P. Yang, and E. K. Wakeland. 1998. Genetic dissection of SLE pathogenesis: Sle1 on murine chromosome 1 leads to a selective loss of tolerance to H2A/H2B/DNA subnucleosomes. *J. Clin. Invest. 101: 1362.*
34. Ishikawa, S., T. Sato, M. Abe, S. Nagai, N. Onai, H. Yoneyama, Y. Zhang, T. Suzuki, S. Hashimoto, T. Shirai, M. Lipp, and K. Matsushima. 2001. Aberrant high expression of B lymphocyte chemokine (BLC/CXCL13) by $C11b^+CD11c^+$ dendritic cells in murine lupus and preferential chemotaxis of B1 cells towards BLC. *J. Exp. Med. 193:1393.*
35. Gotoh, Y., H. Takashima, K. Noguchi, H. Nishimura, M. Tokushima, T. Shirai, and M. Kimoto. 1993. Mixed haplotype Abz/Aad class II molecule in (NZB × NZW)F_1 mice detected by T cell clones. *J. Immunol. 150: 4777.*
36. Yoneyama, H., S. Narumi, Y. Zhang, M. Murai, M. Baggiolini, A. Lanzavecchia, T. Ichida, H. Asakura, and K. Matsushima. 2002. Pivotal role of dendritic cell-derived CXCL10 in the retention of T helper cell 1 lymphocytes in secondary lymph nodes. *J. Exp. Med. 195:1257.*
37. Iwasaki, A., and B. L. Kelsall. 2000. Localization of distinct Peyer's patch dendritic cell subsets and their recruitment by chemokines macrophage inflammatory protein (MIP)-3α, MIP-3β, and secondary lymphoid organ chemokine. *J. Exp. Med. 191:1381.*
38. Scheinecker, C., R. McHugh, E. M. Shevach, and R. N. Germain. 2002. Constitutive presentation of a natural tissue autoantigen exclusively by dendritic cells in the draining lymph node. *J. Exp. Med. 196:1079.*
39. Walport, M. J. 2001. Complement. *N. Engl. J. Med. 344:1140.*
40. Adams, S., P. Leblanc, and S. K. Datta. 1991. Junctional region sequences of T-cell receptor β-chain genes expressed by pathogenic anti-DNA autoantibody-inducing helper T cells from lupus mice: possible selection by cationic autoantigens. *Proc. Natl. Acad. Sci. USA 88:11271.*
41. Hori, S., T. Nomura, and S. Sakaguchi. 2003. Control of regulatory T cell development by the transcription factor Foxp3. *Science 299:1057.*
42. Setoguchi, K., Y. Misaki, Y. Araki, K. Fujio, K. Kawahata, T. Kitamura, and K. Yamamoto. 2000. Antigen-specific T cells transduced with IL-10 ameliorate experimentally induced arthritis without impairing the systemic immune response to the antigen. *J. Immunol. 165:5980.*
43. Nakajima, A., C. M. Seroogy, M. R. Sandora, I. H. Tamer, G. L. Costa, C. Taylor-Edwards, M. H. Bachmann, C. H. Contag, and C. G. Fathman. 2001. Antigen-specific T cell-mediated gene therapy in collagen-induced arthritis. *J. Clin. Invest. 107:1293.*
44. Kessels, H. W., M. C. Wolkers, M. D. van den Boom, M. A. van der Valk, and T. N. Schumacher. 2001. Immunotherapy through TCR gene transfer. *Nat. Immunol. 2:957.*
45. Schumacher, T. N. 2002. T-cell-receptor gene therapy. *Nat. Rev. Immunol. 2:512.*

Nicked β_2-glycoprotein I: a marker of cerebral infarct and a novel role in the negative feedback pathway of extrinsic fibrinolysis

Shinsuke Yasuda, Tatsuya Atsumi, Masahiro Ieko, Eiji Matsuura, Kazuko Kobayashi, Junko Inagaki, Hisao Kato, Hideyuki Tanaka, Minoru Yamakado, Minoru Akino, Hisatoshi Saitou, Yoshiharu Amasaki, Satoshi Jodo, Olga Amengual, and Takao Koike

β_2-Glycoprotein I (β_2-GPI) is proteolytically cleaved by plasmin in domain V (nicked β_2-GPI), being unable to bind to phospholipids. This cleavage may occur in vivo and elevated plasma levels of nicked β_2-GPI were detected in patients with massive plasmin generation and fibrinolysis turnover. In this study, we report higher prevalence of elevated ratio of nicked β_2-GPI against total β_2-GPI in patients with ischemic stroke (63%) and healthy subjects with lacunar infarct (27%) when compared to healthy subjects with normal findings on magnetic resonance imaging (8%), suggesting that nicked β_2-GPI might have a physiologic role beyond that of its parent molecule in patients with thrombosis. Several inhibitors of extrinsic fibrinolysis are known, but a negative feedback regulator has not been yet documented. We demonstrate that nicked β_2-GPI binds to Glu-plasminogen with K_D of 0.37×10^{-6} M, presumably mediated by the interaction between the fifth domain of nicked β_2-GPI and the fifth kringle domain of Glu-plasminogen. Nicked β_2-GPI also suppressed plasmin generation up to 70% in the presence of tissue plasminogen activator, plasminogen, and fibrin. Intact β_2-GPI lacks these properties. These data suggest that β_2-GPI/plasmin-nicked β_2-GPI controls extrinsic fibrinolysis via a negative feedback pathway loop. (Blood. 2004; 103:3766-3772)

Introduction

β_2-Glycoprotein I (β_2-GPI), also known as apolipoprotein H, is a phospholipid-binding plasma protein. Phospholipid-bound β_2-GPI is one of the major target antigens for antiphospholipid antibodies[1-3] present in patients with antiphospholipid syndrome (APS), an autoimmune disorder characterized by arterial/venous thrombosis and pregnancy morbidity.[4] β_2-GPI has 5 homologous short consensus repeats, designated as domains I to V. Domains of β_2-GPI structurally resemble each other, except that domain V has an extra C-terminal loop and a positively charged lysine cluster. In 1993, Hunt et al[5] reported that β_2-GPI is proteolytically cleaved between Lys317 and Thr318 in domain V (nicked β_2-GPI), being unable to bind to phospholipids. This cleavage is generated by factor Xa or by plasmin, with plasmin being more effective.[6]

A large number of reports have detailed the in vitro properties of β_2-GPI as a natural anticoagulant/procoagulant regulator by inhibiting phospholipid-dependent reactions, such as prothrombinase and tenase activity on platelets or phospholipid vesicles,[7,8] factor XII activation,[9] and anticoagulant activity of activated protein C.[10,11] Apart from specific hemostatic functions, β_2-GPI activates lipoprotein lipase,[12] lowers the triglyceride level,[13] binds to oxidized low-density lipoprotein to prevent the progression of atherosclerosis,[14] and binds to nonself particles or apoptotic bodies to allow their clearance.[15-17] Little attention has been given to the functions of the nicked form of β_2-GPI because its phospholipid-binding activity was thought to exert the physiologic or pathologic functions of β_2-GPI.

Fibrinolytic reactions involve the formation of plasmin from the zymogen plasminogen and the hydrolytic cleavage of fibrin to fibrin degradation products by plasmin. Plasminogen, a 92-kDa glycoprotein, is present in plasma at a concentration of approximately 2 μM.[18] Plasminogen consists of 7 domains: one N-terminal peptide, 5 kringle domains bearing a lysine-binding site (LBS) with the capacity to bind fibrin as well as antifibrinolytic proteins carrying lysine, and one serine protease domain.[19] Plasmin conversion from plasminogen by tissue plasminogen activator (tPA) is a key event in extrinsic fibrinolysis for the thrombolysis against intravascular blood clots. Plasmin is one of the most potent enzymes and has a variety of biologic activities; thus, the regulation of plasmin generation and activity is important to maintain the homeostatic balance in vivo. In particular, an excess of fibrinolytic activity can lead to life-threatening bleeding events. Physiologic inhibitors of extrinsic fibrinolysis include α_2-antiplasmin (α_2-AP)[20] and plasminogen activator inhibitor 1 (PAI-1).[21] These inhibitors regulate fibrinolysis through different mechanisms.

Nicked β_2-GPI has been identified by sandwich enzyme-linked immunosorbent assay (ELISA) in plasma of patients with disseminated intravascular coagulation (DIC)[22] or leukemia,[23] both conditions characterized by massive thrombin generation and fibrinolytic

From the Department of Medicine II, Hokkaido University Graduate School of Medicine, Sapporo, Japan; Department of Internal Medicine, School of Dentistry, Health Sciences University of Hokkaido, Ishikari-Tobetsu, Hokkaido, Japan; Department of Cell Chemistry, Institute of Molecular and Cellular Biology, Okayama University Medical School, Okayama, Japan; National Cardiovascular Center Research Institute, Osaka, Japan; Narita R&D Center, Iatron laboratories Inc, Mito, Chiba, Japan; Department of Medicine, Mitsui Memorial Hospital, Tokyo, Japan; Department of Neurosurgery, Azabu Neurosurgical Hospital, Sapporo, Japan.

Submitted August 7, 2003; accepted January 5, 2004. Prepublished online as *Blood* First Edition Paper, January 15, 2004; DOI 10.1182/blood-2003-08-2712.

Supported in part by grants from the Japanese Ministry of Health, Labour and Welfare, by those from the Japanese Ministry of Education, Culture, Sports, Science and Technology, and by the Sankyo Foundation of Life Science.

Reprints: Tatsuya Atsumi, Department of Medicine II, Hokkaido University Graduate School of Medicine, N15, W7, Kita-ku, Sapporo 060-8638, Japan; e-mail: at3tat@med.hokudai.ac.jp.

The publication costs of this article were defrayed in part by page charge payment. Therefore, and solely to indicate this fact, this article is hereby marked "advertisement" in accordance with 18 U.S.C. section 1734.

turnover. To investigate the biologic and clinical significance of nicked β_2-GPI in a disease characterized by a lower level of thrombin generation and fibrin turnover than DIC, we evaluated the cleavage ratio of β_2-GPI in plasma of patients with ischemic stroke and the results are presented herein. Further, we investigated the role of nicked β_2-GPI in extrinsic fibrinolysis and demonstrate for the first time that nicked β_2-GPI binds to plasminogen. We also describe the inhibitory effect of nicked β_2-GPI on the fibrin surface where plasminogen is proteolytically activated into plasmin. Because β_2-GPI may be cleaved in vivo by plasmin during thrombus formation and thrombolysis, these phenomena represent a novel negative feedback loop in extrinsic fibrinolysis where β_2-GPI plays a key role.

Patients, materials, and methods

Study patients

The study population comprised 62 patients with history of ischemic stroke diagnosed by magnetic resonance imaging (MRI) performed at the time of admission to the Azabu Neurosurgical Hospital (female-to-male ratio, 12:50; mean age, 68 ± 9 years). Blood samples were obtained from the patients at least 6 months after their last occlusive event.

We also investigated 130 age- and sex-matched apparently healthy subjects with no history of cerebral infarct who consented to join the study. All subjects underwent a cerebral MRI at the Neuroradiology Department at Mitsui Memorial Hospital and images were analyzed by an experienced neuroradiologist. According to the MRI findings the healthy subjects were divided into 2 groups: 52 with lacunar infarcts (female-to-male ratio, 20:32; mean age 67 ± 9 years) and 78 without any abnormality (female-to-male ratio, 26:52; mean age, 66 ± 6 years). Blood sampling was performed at the same time of the MRI scan. All the patients and healthy volunteers provided informed consent according to Declaration of Helsinki principles.

Blood collection

Venous blood was collected in tubes containing one-tenth volume of 0.105 M sodium citrate and was centrifuged immediately at 4°C. Plasma samples were depleted of platelets by filtration then stored at −70°C until use.

Materials

Monoclonal antibodies. To measure the plasma levels of nicked or total β_2-GPI, we used 2 monoclonal antibodies, 1 monoclonal anti–nicked β_2-GPI antibody (NGPI-60) that specifically reacts against nicked β_2-GPI and the other monoclonal anti-β_2-GPI antibody (NGPI-23) that equally reacts with nicked and intact β_2-GPI.[23]

An IgG mouse monoclonal antihuman β_2-GPI antibody directed to domain III of human β_2-GPI (Cof-22) was used for the purification of nicked β_2-GPI and evaluation of the binding of nicked β_2-GPI to immobilized Glu-plasminogen.[24] Cleavage of β_2-GPI by plasmin did not affect the binding of Cof-22 to β_2-GPI because the epitope of Cof-22 antibody on β_2-GPI molecule resides on domain III (data not shown).

Antihuman plasminogen antibodies directed to kringles 1 to 3 or against kringle 4 were obtained from American Diagnostica (Greenwich, CT).

Proteins. β_2-GPI was purified from human plasma, as described.[25] Nicked β_2-GPI was prepared as reported[26] with slight modifications that included an additional purification step; β_2-GPI was treated with human plasmin (Calbiochem Novabiochem, La Jolla, CA) at 37°C for 3 hours, at a molar ratio of β_2-GPI/plasmin of 8:1. Plasmin-treated β_2-GPI was first purified on a Cof 22–Sepharose column and subsequently on a heparin-Sepharose column. The heparin nonbinding fraction was collected and further purified by ion-exchange chromatography using Mono-Q column (Pharmacia Biotech, Uppsala, Sweden). Purified β_2-GPI was reduced using 2-mercaptoethanol and subjected to sodium dodecyl sulfate–polyacrylamide gel electrophoresis (SDS-PAGE), appearing as a single band smaller than that of the intact one (data not shown).

The domain V–deleted mutant protein (domains I-IV) of β_2-GPI was expressed using a baculovirus system as reported.[24] This mutant β_2-GPI does not include the cleavage site for plasmin.

Glu-plasminogen was purified from the plasma of healthy Japanese donors using chromatography on lysine-Sepharose 4B (Pharmacia Biotech) and diethylaminoethyl (DEAE) Sephadex A-50 (Pharmacia Biotech). Plasminogen kringles 1 to 3 fragment, plasminogen kringle 4 fragment, and mini-plasminogen, which consists of the kringle 5 and serine protease domain of plasminogen, were obtained from Technoclone (Vienna, Austria). Recombinant tPA (2-chain, Duteplase) was obtained from Sumitomo Pharmaceutical (Osaka, Japan). ε-Aminocaproic acid (EACA) was purchased from Sigma Chemical (St Louis, MO).

Methods

Measurement of plasma levels of nicked β_2-GPI. Plasma levels of nicked β_2-GPI were determined by a sandwich ELISA as previously described with slight modifications.[23] Briefly, polystyrene microtiter plates were coated with 100 μL monoclonal anti-nicked β_2-GPI antibody (NGPI-60) in 50 mM Tris (trishydroxymethylaminomethane)–HCL, pH 7.5, containing 0.15 M NaCl and incubated overnight at 4°C. Wells were washed 3 times with 0.5 M NaCl containing 0.05% Tween 20 and 100 μL citrated plasma samples diluted 5-fold in 20 mM Tris-HCl, pH 7.5, containing 0.5 M NaCl and 0.05% Tween 20 (sample buffer) were added. After 2 hours of incubation at room temperature and washing 3 times, 100 μL biotinylated $F(ab')_2$ fragment of monoclonal anti-β_2-GPI (NGPI-23; 2 μg/mL) was added to each well, followed by 1 hour of incubation. Then, 100 μL alkaline phosphatase (ALP)–conjugated streptavidin (Zymed, San Francisco, CA) at a 1:1000 dilution in sample buffer was added to each well. After another 1 hour of incubation and 3 times washing, 200 μL substrate (1 mg/mL p-nitrophenylphosphate disodium [Sigma Chemical] in 1 M diethanolamine buffer [pH 9.8]) was added. Optical density (OD) was read at 492 nm with reference at 620 nm using an ELISA plate reader. The plasma levels of nicked β_2-GPI were determined from a standard curve constructed with citrated plasma spiked with known amounts of purified nicked β_2-GPI.

Measurement of plasma levels of total β_2-GPI. Plasma levels of total β_2-GPI were determined by a sandwich ELISA using F(ab') fragment of NGPI-23 as the capture antibody and biotinylated antihuman β_2-GPI rabbit IgG as the tag antibody as previously reported.[23] Plasma samples of 50 μL (8000-fold diluted) were added to the wells containing the immobilized antibody. The ALP-conjugated streptavidin (Zymed) was then added and bound ALP was determined as described ("Measurement of plasma levels of nicked β_2-GPI"). The amounts of total β_2-GPI in plasma were calculated from a calibration curve constructed with known amounts of purified β_2-GPI. A nicked β_2-GPI ratio was calculated in all samples using the formula: (plasma nicked β_2-GPI/plasma total β_2-GPI) × 1000.

Other laboratory investigations. The same plasma samples were tested for thrombin-antithrombin (TAT) complexes, plasmin-antiplasmin (plasmin inhibitor) complex (PPI), and D-dimers (DDs) by latex agglutination assay using commercial kits LPIAACE TAT, LPIAACE PPI, LPIAACE D-D dimer (Dia-Iatron, Tokyo, Japan), according to the manufacturer's instructions.

ELISA for binding of intact or nicked β_2-GPI to plasminogen. The binding of nicked or intact β_2-GPI was investigated by ELISA. Fifty microliters of Glu-plasminogen (10 μg/mL) in phosphate-buffered saline (PBS), pH 7.4, was distributed in each well of a Sumilon Type S microtiter ELISA plate (Sumitomo Bakelite, Tokyo, Japan) and incubated overnight at 4°C. After washing twice with PBS and blocking with 2% gelatin-PBS for 1 hour at 37°C, 50 μL of serial dilutions of intact or nicked β_2-GPI in 1% bovine serum albumin (Sigma Chemical)–PBS (1% BSA-PBS) were placed in each well. Plates were incubated for 1 hour at room temperature and washed 3 times with PBS containing 0.05% Tween 20 (PBS-Tween), then 50 μL/well Cof-22 (100 ng/mL) in 1% BSA-PBS was distributed. After incubation and washing as above, 50 μL/well of ALP-conjugated anti-mouse IgG (Sigma Chemical), diluted 1:2000 in 1% BSA-PBS, was put into each well, followed by incubation. Substrate (100 μL) was distributed after washing 4 times with PBS-Tween and incubated. OD was read at 405 nm with reference at 620 nm.

The role of plasminogen LBS in binding to nicked β_2-GPI was evaluated by a competitive ELISA adding serial dilutions of EACA, a lysine analog, into the nicked β_2-GPI solution.

Kinetic assay for molecular interaction between nicked β_2-GPI and plasminogen. Real-time analysis for molecular interaction between nicked β_2-GPI and Glu-plasminogen was performed using an optical-biosensor, IAsys system (Affinity Sensors, Paramus, NJ). Biotinylated Glu-plasminogen was immobilized on the wall of a biotin cuvette (Affinity Sensors) via streptavidin (Sigma Chemical). After blocking with 0.01% BSA-PBS and washing with PBS, various concentrations (up to 4 μM) of native or nicked β_2-GPI were placed in the cuvette and ligand bound to the plasminogen-coated surface was detected. Obtained data were fitted using linear regression to find the intercept and gradient. This analysis was used to determine the association rate constant (k_{ass}) and dissociation rate constant (k_{diss}), from the variation of the on-rate constant (k_{on}) with ligand concentration. According to the equation; $k_{on} = k_{diss} + k_{ass}$ [ligand], K_D and K_A are determined as follows; $K_D = k_{diss}/k_{ass}$ and $K_A = k_{ass}/k_{diss}$.

Inhibition ELISA. To identify the nicked β_2-GPI-binding site on Glu-plasminogen, the inhibition of Glu-plasminogen binding by fragments of plasminogen was examined. Fifty microliters of nicked β_2-GPI (0.2 μM) diluted in PBS was put into each well of a MaxiSorp microtiter plate (Nalge Nunc International, Roskilde, Denmark) and incubated overnight at 4°C. After washing twice with PBS and blocking with 2% gelatin-PBS for 1 hour at 37°C, serial dilutions of inhibitor (BSA, plasminogen kringle 1-3, plasminogen kringle 4, or mini-plasminogen) were added (50 μL/well) followed by overnight incubation at 4°C. After washing with PBS-Tween, 10 μg/mL Glu-plasminogen was then added (50 μL/well) and incubated for 30 minutes at room temperature, and plates were washed 3 times with PBS-Tween. To compare the inhibitory effect between kringle 1 to 3 and mini-plasminogen, a monoclonal antikringle 4 antibody (American Diagnostica) was used to detect bound Glu-plasminogen, whereas a monoclonal antikringle 1 to 3 antibody (American Diagnostica) was used to compare the inhibition of mini-plasminogen with that of kringle 4. After incubation with these monoclonal antibodies, bound Glu-plasminogen on nicked β_2-GPI was evaluated by ALP-conjugated antimouse IgG, followed by substrate addition as described ("ELISA for binding of intact or nicked β_2-GPI to plasminogen").

Inhibitory effect of nicked β_2-GPI on the binding of plasminogen to fibrin. To investigate whether nicked β_2-GPI interferes with the binding of Glu-plasminogen to immobilized fibrin in a liquid phase or not, the following experiment was done. Each well of a Sumilon Type S microtiter plate (Sumitomo Bakelite) was coated with soluble fibrin monomer (5 μg/mL) and incubated at 4°C overnight, followed by washing with PBS-Tween and blocking with 2% gelatin-PBS at 37°C. Biotinylated Glu-plasminogen (5 μg/mL in 1% BSA-PBS) was preincubated with different concentrations of intact or nicked β_2-GPI for 1 hour at room temperature and added to the wells in triplicate. After incubation for 1 hour at room temperature, each well was washed with PBS-Tween. ALP-conjugated streptavidin was diluted to 3000 times in PBS and distributed to the wells. After 1 hour of incubation and washing, substrate was added and absorbance was measured as described.

Effects of intact or nicked β_2-GPI on tPA activity: chromogenic assay. In the presence of fibrin, tPA can effectively activate plasminogen to plasmin. Because we speculated that nicked β_2-GPI might interfere with this activation step by binding to plasminogen, chromogenic assay measuring plasmin generation was introduced in the presence of tPA, Glu-plasminogen, fibrin monomer, and β_2-GPI. The effect of intact/nicked β_2-GPI on the activity of plasmin generated was evaluated using a parabolic rate assay. The activity of tPA was measured in a chromogenic assay as described[27] with some modifications. A mixture of the same volume of 50 U/mL tPA in PBS and 1 M acetate buffer (pH 3.9) was incubated for 5 minutes at room temperature, then diluted 1:160 with assay buffer (50 mM Tris-HCl, pH 8.8, 100 mM NaCl, and 0.01% Triton X-100). Then 100 μL of the diluted tPA solution was incubated in a Sumilon Type S microtiter plate with 100 μL detection reagents consisting of Glu-plasminogen and plasmin-sensitive substrate (Glu-plasminogen [70 μg/mL] and 0.6 mM chromogenic substrate S-2251 [Chromogenix, Mölndal, Sweden] in assay buffer) with intact or nicked β_2-GPI and 2 μL/well soluble fibrin monomer (3.3 mg/mL, in 3.5 M urea). The final concentrations of intact/nicked β_2-GPI were 0, 0.25, and 0.5 μM. Domain I to IV of β_2-GPI mutant or BSA served as the negative control. After incubation at 37°C for 12 hours, the activity of plasmin generated was determined by measuring absorbance at 405 nm using a microplate reader (model 3550; BioRad, Hercules, CA). A standard curve was generated using serial dilutions of tPA. The plasmin generation in this system was expressed as corresponding tPA activity (U/mL).

Effects of intact or nicked β_2-GPI on tPA activity: fibrin plate assay. To exclude the possibility that nicked β_2-GPI affected S-2251 cleavage without interacting with fibrinolytic factors, fibrinolysis was evaluated by conventional fibrin plate assays. Fibrin was layered on a plastic plate 10 cm in diameter, using the same volumes of 0.2% plasminogen-free fibrin (Sigma Chemical), 1% agarose, and 200 μL/plate thrombin, 20 U/mL. Then, 6 μL of the diluted tPA solution ("Effects of intact or nicked β_2-GPI on tPA activity: chromogenic assay") was incubated with the same volume of Glu-plasminogen (70 μg/mL) in assay buffer, with intact or nicked β_2-GPI (up to 0.5 μM). After 36 hours of incubation at 37°C, the area of lysis rings was measured. A standard curve was generated from serial dilutions of tPA.

Statistical analysis. Statistical evaluation was performed by the *t* test, Fisher exact test, χ^2 test, or Spearman rank correlation as appropriate. *P* values less than .05 were considered statistically significant.

Results

Levels of nicked β_2-GPI in plasma samples

The plasma levels of nicked β_2-GPI ratio are shown in Figure 1. A normal level of nicked β_2-GPI ratio was derived from the apparently healthy subjects without any MRI abnormality, the mean plus 1 SD representing the upper limit of normal. A higher prevalence of elevated nicked β_2-GPI ratio was found in patients with ischemic stroke (63%, 39 of 62) and healthy subjects with lacunar infarct (27%, 14 of 52) when compared to healthy subjects with normal MRI findings (8%, 6 of 78). Relative risks of having stroke or asymptomatic lacunar infarction were approximated by odds ratio (95% CI), 20.3 (7.6-54.2) and 4.4 (1.6-12.4), respectively.

The prevalence of elevated levels of markers of thrombin generation and fibrinolytic turnover in our population are shown in Figure 2. A statistically significant correlation was observed between levels of PPI and nicked β_2-GPI ratio in plasma of healthy subjects with lacunar infarct ($r^2 = 0.31$, $P = .02$). No correlations were found between nicked β_2-GPI ratio and DDs or TAT complexes in any of the groups.

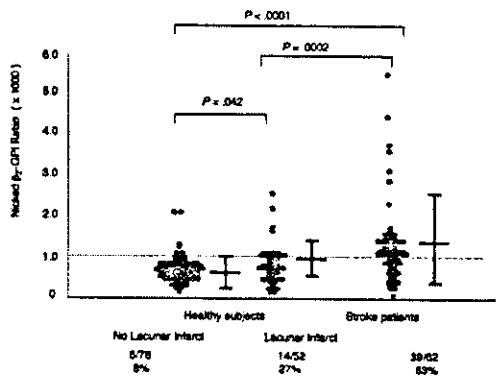

Figure 1. Plasma levels of nicked β_2-GPI. Total and nicked β_2-GPI plasma levels were determined by ELISA. A nicked β_2-GPI ratio, (plasma nicked β_2-GPI/plasma total β_2-GPI) × 1000, was established in all the samples. The dashed line indicates the mean + 1 SD of the ratio in healthy subjects without lacunar infarct. *P* values were calculated using *t* test.

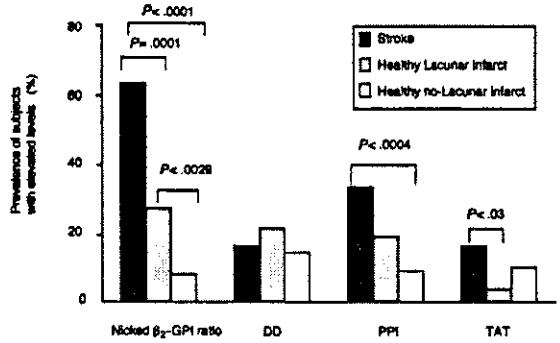

Figure 2. Prevalence of abnormally elevated plasma levels of nicked β_2-GPI and of markers of thrombin generation/fibrinolytic turnover in our population. Plasma levels of D-dimers (DD), plasmin-antiplasmin complex (PPI), and thrombin-antithrombin complexes (TAT) were determined in all the subjects as described in "Patients, materials, and methods."

In the apparently healthy subjects group (n = 130), plasma nicked β_2-GPI ratio significantly correlated with age ($r^2 = 0.483$, $P < .0001$; Figure 3). Therefore, plasma measurement of nicked β_2-GPI might be a useful screening tool in the assessment of patients at risk of ischemic stroke.

Binding of nicked β_2-GPI to Glu-plasminogen

The binding of up to 0.4 μM nicked β_2-GPI to solid-phase Glu-plasminogen occurred in a dose-dependent manner, whereas the same concentrations of intact β_2-GPI did not bind to Glu-plasminogen (Figure 4A). The binding of Cof-22 to β_2-GPI was not affected by the cleavage of β_2-GPI. Molecular interaction between intact or nicked β_2-GPI and plasminogen was investigated using an optical biosensor. Nicked β_2-GPI showed a large extent of binding to immobilized Glu-plasminogen, whereas intact β_2-GPI did not show any specific binding (Figure 4B). The data of k_{on} at different concentrations of nicked β_2-GPI were fitted using linear regression, determining k_{ass} as 0.0006 $M^{-1}s^{-1}$ and k_{diss} as 0.0022 s^{-1} (Figure 4C). Accordingly, K_D and K_A were determined as 0.37×10^{-6} M and 2.70×10^6 M^{-1}, respectively.

Inhibition of binding of Glu-plasminogen to nicked β_2-GPI by the fragments of plasminogen or by EACA

The binding of Glu-plasminogen (10 μg/mL) to immobilized nicked β_2-GPI, but not to native β_2-GPI, was demonstrated by ELISA. For the inhibition assay, the fragments of plasminogen (mini-plasminogen or kringle 4) as the inhibiting factors were added to the wells coated with nicked β_2-GPI, and bound Glu-plasminogen was detected using a monoclonal antikringle 1 to 3 antibody. Mini-plasminogen, but not kringle 4, inhibited the binding between Glu-plasminogen and nicked β_2-GPI (Figure 5A). Kringle 1 to 3 fragment or mini-plasminogen was added as inhibitor and bound Glu-plasminogen was detected using a monoclonal antikringle 4 antibody. Glu-plasminogen binding to nicked β_2-GPI was dose dependently inhibited by mini-plasminogen but not by kringle 1 to 3 fragment (Figure 5B). The fifth domain or the catalytic domain of Glu-plasminogen, therefore, was predicted to mediate its binding to nicked β_2-GPI.

When the binding of nicked β_2-GPI (10 μg/mL) to solid-phase Glu-plasminogen was tested in the presence of different concentrations of EACA, the binding between nicked β_2-GPI and immobilized Glu-plasminogen was abolished in a dose-dependent manner (Figure 5C). Accordingly, LBS on plasminogen might mediate the binding of nicked β_2-GPI to Glu-plasminogen.

Binding of plasminogen to fibrin interfered with by nicked β_2-GPI

We also investigated whether nicked β_2-GPI has an effect on the binding of Glu-plasminogen to immobilized fibrin monomer using an ELISA system. After preincubation with nicked β_2-GPI, but not with intact β_2-GPI, Glu-plasminogen showed decreased binding activity to soluble fibrin monomer (Figure 5D).

Effects of nicked β_2-GPI on extrinsic fibrinolysis

The amidolytic activity of newly generated plasmin was evaluated as tPA activity (U/mL) in a chromogenic assay. The activity increased with the concentration of tPA (data not shown). When nicked β_2-GPI was added, the tPA activity decreased in a dose-dependent manner (Figure 6A). Intact β_2-GPI at 0.25 μM did not suppress the fibrinolytic activity, whereas intact β_2-GPI in a higher concentration (0.50 μM) slightly suppressed the fibrinolytic activity. The same amount of BSA or the recombinant domain I to IV of β_2-GPI did not affect the tPA activity.

The fibrinolytic activity of generated plasmin was measured as tPA activity (U/mL) in a fibrin plate assay. Fibrinolytic activity was suppressed by nicked β_2-GPI at 0.25 and 0.50 μM. Intact β_2-GPI at 0.50 μM also slightly inhibited the fibrinolytic activity. However, 0.25 μM intact β_2-GPI did not affect the fibrinolytic activity of tPA (Figure 6B).

Discussion

In the first part of this study, we demonstrated that plasma levels of nicked β_2-GPI were elevated in patients with ischemic stroke, indicating an elevated degree of fibrin turnover, but lower than that of DIC where thrombin and plasmin are massively generated.

In fact, nicked β_2-GPI was detected in large quantities in plasma of patients with DIC, a pathologic state characterized by marked increase of plasma PPI.[22] We observed a strong correlation between plasma levels of nicked β_2-GPI and those of PPI in the healthy individuals showing lacunar infarcts on MRI, suggesting that nicked β_2-GPI may rather reflect "minor" plasmin generation. In the presence of larger plasmin generation, the correlation between nicked β_2-GPI and PPI may be lost,[23] presumably due to the consumption of α_2-AP. In individuals with MRI abnormalities the prevalence of increased nicked β_2-GPI ratio was higher than that of PPI, DDs, and TAT complexes (46%, 27%, 19%, and 11%, respectively). Thus, the detection of nicked β_2-GPI may

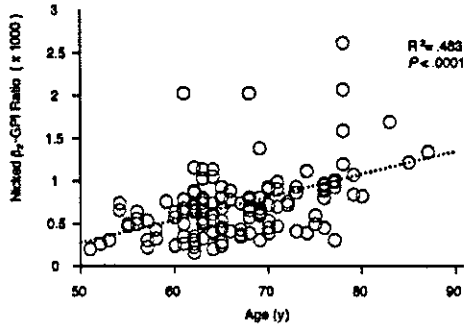

Figure 3. Correlation between plasma levels of nicked β_2-GPI and age in apparently healthy subjects. Nicked β_2-GPI was measured by a sandwich ELISA. The dotted line represents the regression curve. Each circle shows nicked β_2-GPI ratio and age in each subject.

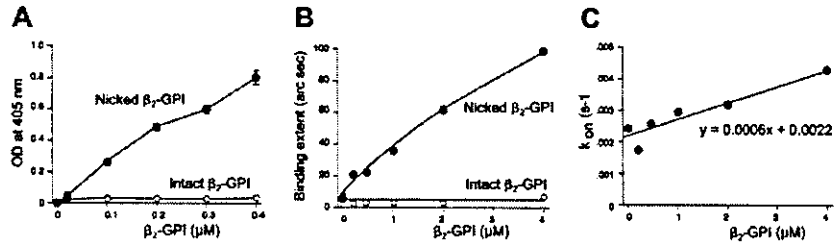

Figure 4. Binding of intact/nicked β_2-GPI to Glu-plasminogen. (A) Binding of intact or nicked β_2-GPI to immobilized Glu-plasminogen was evaluated by ELISA using mouse monoclonal anti-β_2-GPI antibody Cof-22. Closed circles indicate the dose-dependent binding of nicked β_2-GPI to Glu-plasminogen, whereas open circles indicate that intact β_2-GPI is unable to bind to Glu-plasminogen. (B-C) Kinetic plot showing molecular interaction between Glu-plasminogen and intact or nicked β_2-GPI. Intact β_2-GPI or nicked β_2-GPI binding to Glu-plasminogen was detected using IAsys, an optical biosensor as described in "Patients, materials, and methods." Binding extent (arc sec) was compared between intact and nicked β_2-GPI (B). Obtained on-rate constant (k_{on}) for nicked β_2-GPI was plotted and fitted using linear regression to find the intercept and gradient (C). A formula for determining the association rate constant (k_{ass}) and dissociation rate constant (k_{diss}) is as follows: $k_{on} = k_{diss} + k_{ass}$ [ligand]. Error bars indicate SDs.

represent a more sensitive marker of vascular lesions than PPI, DDs, or TAT complexes.

In support of this concept is the correlation between nicked β_2-GPI ratio and age in the apparently healthy subjects, suggesting that "minor" plasmin generation might be associated with subclinical or early clinical atherosclerosis. It is widely accepted that atherosclerosis is associated with endothelial cell activation and minor plaque rupture leading to small thrombus formation, secretion of t-PA, and plasmin generation, ultimately cleaving β_2-GPI. Indeed, nicked β_2-GPI can be generated on the surface of activated endothelial cells or platelets.[23]

In the second part of this study, we investigated the properties of nicked β_2-GPI in vitro to evaluate the biologic significance of our observations. We showed that nicked β_2-GPI specifically binds to Glu-plasminogen and inhibits extrinsic fibrinolysis in vitro. In contrast, neither domain I to IV of β_2-GPI nor intact β_2-GPI revealed such functions. The administration of intact β_2-GPI in higher concentrations also suppressed plasmin generation, perhaps owing to the nicked β_2-GPI produced by the newly generated plasmin. Under clinical conditions characterized by massive plasmin generation such as DIC or acute thrombosis, plasmin is generated by tPA released from activated endothelial cells with thrombus formation, and plasmin cleaves β_2-GPI on the thrombus, changing the properties of β_2-GPI. We propose that β_2-GPI is a precursor of plasmin-nicked β_2-GPI, a physiologic inhibitor of fibrinolysis.

The crystal structure of human β_2-GPI has been defined.[28,29] Bouma et al[28] proposed that a large positively charged patch in domain V binds to anionic surfaces with a flexible and partially hydrophobic loop inserted into the lipid layer. According to the conformation of the nicked domain V, as predicted from the x-ray structure of the intact domain V and confirmed by heteronuclear magnetic resonance, the nicked C-terminal loop is tightly fixed by electrostatic interaction with enhanced stability, the result being neutralization of the positive charge of the lysine cluster.[26,30]

Glu-plasminogen, a full-length protein, is the naturally circulating form of plasminogen. Kringle 5 of Glu-plasminogen has a higher affinity for intact fibrin.[31,32] LBS in kringle 5 of Glu-plasminogen mediates its binding to N-terminal lysine on fibrin, an event essential to initiate fibrinolysis reactions. This initial binding of Glu-plasminogen to fibrin induces a conformational change from a "closed" to an "open" form, thus promoting accessibility to plasminogen activators such as tPA or urokinase.[19] On the fibrin surface, generated plasmin cleaves the single-chain tPA into the 2-chain tPA, a more active form, providing a positive feedback for plasmin generation. Plasmin simultaneously degrades fibrin and makes C-terminal lysine of fibrin more accessible to plasminogen via kringles 1,[33,34] 2, and 3,[35] thus accelerating fibrinolysis.

According to the results of the inhibition studies using plasminogen fragments or EACA (Figure 5), and comparison of the effect on plasmin generation between nicked β_2-GPI and domain I to IV of β_2-GPI (Figure 6A), it would be indicated that the binding of nicked β_2-GPI to Glu-plasminogen is mediated by the interaction between the lysine-cluster patch in domain V of the nicked β_2-GPI and LBS on the plasminogen kringle 5,[36] although it still may be possible that an excess amount of EACA interacts with the catalytic domain of Glu-plasminogen. The conformational difference between intact and nicked β_2-GPI is critical for its binding to

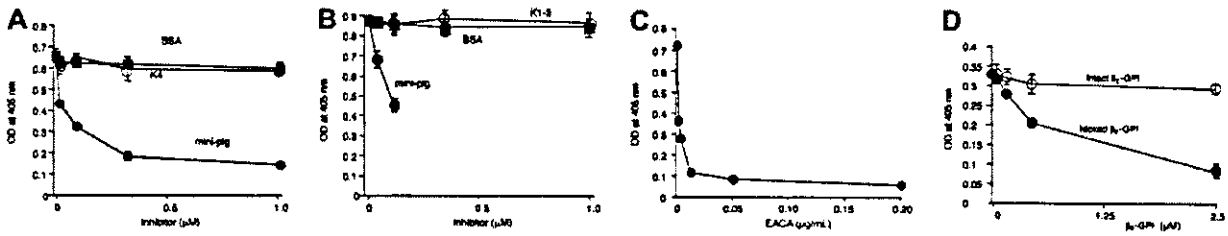

Figure 5. Identification of the binding site of Glu-plasminogen to β_2-GPI by inhibition ELISA using plasminogen fragments. (A) Binding of Glu-plasminogen to immobilized nicked β_2-GPI was tested by ELISA in the presence of possible inhibitors. After nicked β_2-GPI immobilization onto microtiter plates, different concentrations of kringle 4 of plasminogen (○) or mini-plasminogen (that consists of kringle 5 and catalytic domain of plasminogen; ●) were added as inhibitors. BSA (■) served as control. After incubation and washing, Glu-plasminogen (10 μg/mL) was added and bound Glu-plasminogen was determined using kringle 1- to 3-specific mouse monoclonal antiplasminogen antibody. (B) For the inhibition ELISA kringle 1 to 3 of plasminogen (○) or mini-plasminogen (●) served as inhibitors. Glu-plasminogen bound to immobilized β_2-GPI was detected using kringle 4-specific mouse monoclonal antiplasminogen antibody. Assays were run in triplicate. (C) Competitive ELISA using EACA, a lysine homologue. Binding of nicked β_2-GPI (0.2 μM) to immobilized Glu-plasminogen was tested by ELISA using Cof-22 antibody in the presence of various concentrations of EACA (0-0.20 μg/mL). (D) Soluble fibrin monomer (5 μg/mL) was coated on the surface of a microtiter plate and blocked. Biotinylated Glu-plasminogen (5 μg/mL) was preincubated with intact or nicked β_2-GPI and added to the wells. After incubation and washing, ALP-conjugated streptavidin was used for detection. Assays were run triplicate. Error bars indicate SDs. K indicates kringle; mini-plg, mini-plasminogen.

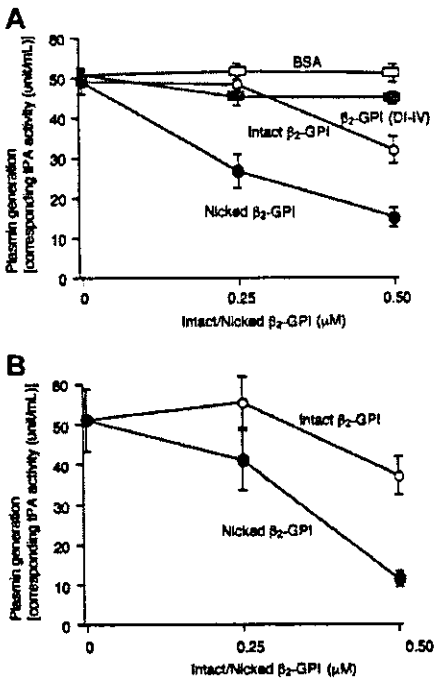

Figure 6. Inhibitory effect of nicked β_2-GPI on plasmin generation. (A) Plasmin generation was measured by parabolic rate assay using synthetic substrate S-2251 in the presence of tPA, Glu-plasminogen, and fibrin monomer. Nicked β_2-GPI (●), intact β_2-GPI (○), β_2-GPI domain I-IV mutant (■), or BSA (□) was added to the reaction in the indicated concentrations. After 12 hours of incubation, absorbance at 405 nm was measured and expressed as tPA activity (U/mL) using tPA as standard. (B) Fibrinolytic activity was measured using fibrin plate assay. Solution reaction containing tPA, Glu-plasminogen, and nicked (●) or intact β_2-GPI (○) were placed onto fibrin plates. After 36 hours of incubation, the ring area of lysis was measured. Assays were performed in triplicate. Error bars indicate SDs. D indicates domain.

phospholipid or plasminogen. The lysine-cluster patch in domain V of nicked β_2-GPI may gain accessibility for the LBS of Glu-plasminogen, whereas the C-terminal loop of intact β_2-GPI may interfere with interactions of LBS and the Glu-plasminogen kringle 5.

The fibrinolytic system is regulated at different levels, either at plasminogen activation or at enzymatically active plasmin. Many factors, including α_2-AP, α_2-macroglobulin, α_1-antitrypsin, inactivated C1, PAI-1, and PAI-2, prevent the overactivation of the fibrinolytic system. The most potent inhibitors are α_2-AP and PAI-1[37]; the former binds to a component of kringle 1 to 3 of plasminogen[38] and can neutralize the generated plasmin more rapidly than α_2-macroglobulin.

Fibrinolysis initiates on binding of kringle 5 of plasminogen to lysine residues on fibrin followed by the binding of kringle 1 to 3 of plasminogen to lysine residues on the cleaved fibrin. α_2-AP does not bind to kringle 5 of plasminogen, hence, does not seem to affect the first interaction. Based on the observation that nicked β_2-GPI interferes the binding between Glu-plasminogen and fibrin monomer (Figure 5D), it is likely that the binding of nicked β_2-GPI to Glu-plasminogen affects the first step of fibrinolysis at least and exerts an inhibitory function in the fibrinolytic system via different mechanisms from that of α_2-AP.

In conclusion, first we have demonstrated that plasma levels of nicked β_2-GPI can be a sensitive marker of cerebral ischemic events and we suggest that plasma measurement of nicked β_2-GPI might be a useful screening tool in the assessment of patients at risk of ischemic stroke. Second, we propose that nicked β_2-GPI is a physiologic inhibitor of fibrinolysis and that plasmin cleavage of β_2-GPI is part of the negative feedback pathway of extrinsic fibrinolysis.

Acknowledgment

We wish to thank Professor Koji Suzuki, from Department of Molecular Pathobiology, Mie University School of Medicine, Tsu, Japan, for great suggestions and fruitful discussions.

References

1. Galli M, Comfurius P, Maassen C, et al. Anticardiolipin antibodies (ACA) directed not to cardiolipin but to a plasma protein cofactor. Lancet. 1990;335:1544-1547.
2. McNeil HP, Simpson RJ, Chesterman CN, Krilis SA. Anti-phospholipid antibodies are directed against a complex antigen that induces a lipid-binding inhibitor of coagulation: β2-glycoprotein I (apolipoprotein H). Proc Natl Acad Sci U S A. 1990;87:4120-4124.
3. Matsuura E, Igarashi Y, Fujimoto M, Ichikawa K, Koike T. Anticardiolipin cofactor(s) and differential diagnosis of autoimmune disease. Lancet. 1990; 336:177-178.
4. Hughes GRV. The antiphospholipid syndrome: ten years on. Lancet. 1993;342:341-344.
5. Hunt JE, Simpson RJ, Krilis SA. Identification of a region of β2-glycoprotein I critical for lipid binding and anti-cardiolipin antibody cofactor activity. Proc Natl Acad Sci U S A. 1993;90:2141-2145.
6. Ohkura N, Hagihara Y, Yoshimura T, Goto Y, Kato H. Plasmin can reduce the function of human β2 glycoprotein I by cleaving domain V into a nicked form. Blood. 1998;91:4173-4179.
7. Nimpf J, Bevers EM, Bomans PHH, et al. Prothrombinase activity of human platelets inhibited by β2-glycoprotein I. Biochem Boiphys Acta. 1986;884:142-149.
8. Shi W, Chong BH, Hogg PJ, Chesterman CN. Anticardiolipin antibodies block the inhibition by β2-glycoprotein I of the factor Xa generating activity of platelets. Thromb Haemost. 1993;70:342-345.
9. Schousboe I, Rasmussen MS. Synchronized inhibition of the phospholipid mediated autoactivation of factor XII in plasma by β2-glycoprotein I and anti-β2-glycoprotein I. Thromb Haemost. 1995; 73:798-804.
10. Mori T, Takeya H, Nishioka J, Gabazza EC, Suzuki K. β2-Glycoprotein I modulates the anticoagulant activity of activated protein C on the phospholipid surface. Thromb Haemost. 1996;75: 49-55.
11. Ieko M, Ichikawa K, Triplett DA, et al. β2-Glycoprotein I is necessary to inhibit protein C activity by monoclonal anticardiolipin antibodies. Arthritis Rheum. 1999;42:167-174.
12. Nakaya Y, Schaefer EJ, Brewer HBJ. Activation of human post heparin lipoprotein lipase by apolipoprotein H (β2-glycoprotein I). Biochem Biophys Res Commun. 1980;95:1168-1172.
13. Wurm H, Beubler E, Polz E, Holasek A, Kostner G. Studies on the possible function of β2-glycoprotein-I: influence in the triglyceride metabolism in the rat. Metabolism. 1982;31:484-486.
14. Hasunuma Y, Matsuura E, Makita Z, Katahira T, Nishi S, Koike T. Involvement of β2-glycoprotein I and anticardiolipin antibodies in oxidatively modified low-density lipoprotein uptake by macrophages. Clin Exp Immunol. 1997;107:569-573.
15. Chonn A, Semple SC, Cullis PR. β2 glycoprotein I is a major protein associated with very rapidly cleared liposomes in vivo, suggesting a significant role in the immune clearance of "non-self" particles. J Biol Chem. 1995;270:25845-25849.
16. Manfredi AA, Rovere P, Galati G, et al. Apoptotic cell clearance in systemic lupus erythematosus; I: opsonization by antiphospholipid antibodies. Arthritis Rheum. 1998;41:205-214.
17. Manfredi AA, Rovere P, Heltai S, et al. Apoptotic cell clearance in systemic lupus erythematosus; II: role of β2-glycoprotein I. Arthritis Rheum. 1998;41:215-223.
18. Wallen P, Wiman B. Characterization of human plasminogen; I: on the relationship between different molecular forms of plasminogen demonstrated in plasma and found in purified preparations. Biochim Biophys Acta. 1970;221:20-30.
19. Ponting CP, Holland SK, Cederholm-Williams SA, et al. The compact domain conformation of human Glu-plasminogen in solution. Biochim Biophys Acta. 1992;1159:155-161.
20. Aoki N, Saito H, Kamiya T, Koie K, Sakata Y, Kobakura M. Congenital deficiency of α2-plasmin inhibitor associated with severe hemorrhagic tendency. J Clin Invest. 1979;63:877-884.
21. Loskutoff DJ, Sawdey M, Mimuro J. Type 1 plasminogen activator inhibitor. Prog Hemost Thromb. 1989;9:87-115.
22. Horbach DA, van Oort ET, Lisman T, Meijers JC,